PARAMETRIC SCREENING OF HYBRID POWERTRAIN ARCHITECTURES FOR HIGH-ENERGY LASER VEHICLES: APPLICATION TO FOXHOUND AND BOXER

Rupert Tull de Salis[1], PE, MEng, MSc

[1]ZeBeyond Ltd, Leamington Spa, UK

ABSTRACT

The US Army and several NATO allies have committed funds for directed energy weapons including high energy lasers (HEL), which require substantial electrical power. Silent Mobility and Silent Watch requirements mandate hybridisation, which also provides the electrical capacity needed for a HEL.

This paper introduces a HEL framework of classes A-E based on target types and fluence physics. It estimates installed HEL mass and power demand by class, and applies rapid powertrain screening to hypothetical hybrid variants of the UK vehicles Foxhound and Boxer. Results show that HELs up to Class B (60 kW) and D (300 kW) laser output can be supported with minimal powertrain modifications by Foxhound and Boxer respectively, and upgrades to support Class C (150 kW) and E (500 kW) are containable within the payload of each vehicle. A rapid methodology is presented to determine what powertrain architecture is needed to support a given HEL.

1. INTRODUCTION

Directed energy weapons (DEW) in high energy laser form (HEL) offer a compelling answer to the rise of aerial drone warfare; a marginal cost per engagement, an unlimited magazine, and a sustained engagement rate far exceeding that of missile systems. [1] However HELs are heavy, and their electrical power requirements are too large for existing vehicle platforms to support without extensive modification. Future vehicle platforms are likely to feature diesel-electric hybrid powertrains in order to support Silent Watch and Silent Mobility functions, with the result that they will naturally include suitable subsystems (inverter, generator) to supply HEL power. The challenge addressed here is planning a future vehicle platform to support a HEL, while many variable parameters affecting the weight and power requirements of the HEL are still in flux.

The U.S. Army has invested substantially in vehicle-mounted HEL systems, including the 50 kW DE M-SHORAD on the Stryker and the 300 kW-class IFPC-HEL programme [11]. The UK's Strategic Defence Review of June 2025 committed nearly £1 billion to directed energy capability across the armed forces, encompassing both laser and electromagnetic systems, and in November 2025 the Ministry of Defence ordered DragonFire laser systems for the Royal Navy [2],[3],[4],[5],[6],[7]. Land applications have followed; the High-Energy Laser Weapon System (HELWS) was demonstrated on a Wolfhound 6×6 armoured vehicle at Porton Down in July 2024 [6][7], and the British Army tested a Radio Frequency Directed Energy Weapon (RFDEW) against drone swarms in Wales in December 2024. [7] In June 2025 the Ministry of Defence issued a market engagement notice for vehicle-mounted laser DEW solutions, with a budget of £20 million and a requirement for deployment within twelve months of contract award.[8] Outside NATO (North Atlantic Treaty Organisation), vehicle-mounted HEL programmes in the 30–100 kW class are in advanced development; the Chinese Silent Hunter mobile ground system is reported at TRL (Technology Readiness Level) 7–8 [1].

Artillery doctrine distinguishes between the maximum rate of fire (for a short burst) and the sustained rate of fire maintainable indefinitely [10]. Congressional Research Service (CRS) Report R46925 [11] identifies analogous constraints for HEL systems: they can engage only one target at a time, require several seconds of continuous dwell to disable each target, and require further time to slew and re-acquire a subsequent target. A further constraint, thermal recovery time, is not quantified in published sources for vehicle HEL systems, but in practice it is dominant: waste heat accumulated during a firing burst may require significant time for cooling, limiting how frequently the weapon can fire. Recent commentary confirms that this is the main rate-limiting constraint of current HEL systems, but it appears that no formal framework exists to characterise it. A new metric is proposed to characterise the rate-of-fire constraints for a HEL system. The Sustained Firing Fraction (SFF, per cent) is proposed for the maximum sustainable ratio of firing time to total time, limited in the best case by the dwell time and re-engagement time, but determined in practice by the cooling of the system. Further metrics seem necessary for maximum engagements per hour, or firing fraction during a burst, but these are affected by the firing time needed for each target, which in practice would be variable owing to target type, engagement distance and atmospheric conditions among other factors, rendering such metrics meaningless. The term SFF is new; its

introduction here is intended to provide a framework for characterizing HEL system requirements for the purpose of sizing hybrid powertrain architectures. Knowing the SFF, along with laser output power and efficiency metrics, it is possible to estimate the average power required from the vehicle platform during sustained engagement.

This parameter strongly influences both the weight and the electrical power requirements of the HEL. A supporting vehicle must not only have sufficient payload for the HEL, but must also supply sufficient electrical power for engagement. The power requirement varies greatly as a function of SFF and other HEL parameters, which are unlikely to be frozen at the time of specifying the vehicle platform. Powertrain design for a HEL platform therefore presents a multi-dimensional optimization problem at the planning stage, with HEL parameters as important inputs.

Published simulations of military and off-road hybrid powertrains rely predominantly on high-fidelity tools for this type of optimization problem, for example ADvanced VehIcle SimulatOR (ADVISOR), Powertrain System Analysis Toolkit (PSAT), Autonomie, and AVL CRUISE. These tools require detailed input data such as engine fuel consumption maps and component efficiency tables. Several sources state that powertrain architecture selection requires complex analysis, large computation times, powertrain simulation expertise and laborious data-gathering. [12],[13], [14],[15], [16], which is not containable in the early phases of planning a new vehicle programme. By contrast, the method presented here can be completed in hours rather than weeks, requires only limited vehicle parameters, which are typically available in open-source programme documents at the concept stage, and does not require dedicated powertrain simulation expertise. This efficiency is particularly valuable when comparing multiple scenarios simultaneously, as in the case of matching a new, partially defined HEL system to a new hybrid vehicle platform.

The data referenced in this paper is drawn entirely from publicly available sources. It should be noted that more accurate information is probably available within restricted sources, that could be used to repeat this analysis with improved assumptions.

2. TACTICAL WHEELED VEHICLE PLATFORMS

The British Army operates a range of protected tactical wheeled vehicles that might serve as hosts for vehicle-mounted HEL systems with hybrid powertrains. The principal available vehicles are described briefly below; two are then selected for primary analysis, as surrogates for hypothetical future platforms. They all use non-hybrid powertrains today, that run on JP-8 (Jet Propellant 8) military diesel fuel.

Foxhound LPPV. The Foxhound Light Protected Patrol Vehicle (LPPV), has a gross vehicle mass (GVM) of 7,500 kg and a stated maximum payload of approximately 2,000 kg. It is powered by a Steyr M16-Monoblock diesel engine rated at 160 kW. [17] It is the smallest British Army vehicle that might support a HEL. [18][19]

Wolfhound 6×6. The Wolfhound Heavy Protected Patrol Vehicle (HPPV), a Mastiff variant manufactured by Force Protection Europe.[20],[21] It has a Caterpillar C7 diesel engine developing 246 kW. [21] It was the host vehicle for the 2024 HELWS live-fire trial of a 15kW HEL at Porton Down [6][7]. It is not selected for primary analysis because it is a transitional platform rather than a planned future programme, and its engine and payload are between Foxhound

and Boxer, which represent the extremes of the UK Army range.

Boxer MIV 8×8. The Boxer Mechanised Infantry Vehicle (MIV) is the British Army's new protected 8×8 wheeled vehicle, with 623 vehicles on order under a £2.8 billion contract [22][23][24]. It has a gross vehicle weight of 38,500 kg and is powered by an MTU diesel rated at 600 kW [25], giving 79 % more power than the Caterpillar C9 installed in the US Army's Stryker A1, and more than twice the power of the Wolfhound. [21] A common drive module carries interchangeable mission modules, leaving a payload of 15,000 kg. A dedicated HEL mission module would be the natural integration method for a Boxer-based laser system, isolating the weapon's power conditioning, thermal management, and energy storage within a self-contained unit that can use power from the drive module's powertrain. The German Bundeswehr has ordered 19 Rheinmetall Skyranger 30 HEL systems, with a stated near-term output target of 50 kW, on Boxer chassis [26].

Jackal 2. The Supacat Jackal 2 (HMT 400) has a GVM of approximately 7,500 kg and a payload broadly comparable to Foxhound, with a Cummins 6.7L diesel engine delivering 134 kW, but it is an open-cab vehicle without the protection level required for operations in contested airspace

MAN HX 8×8. The MAN HX 8×8 logistics truck has been demonstrated as a host for Rheinmetall's 50 kW containerised HEL system, but it is a logistic vehicle and not a protected combat platform.

Vehicle Selection. This paper selects Foxhound and Boxer as the two primary analysis platforms. They represent opposite extremes of the UK Army's protected wheeled vehicle fleet in terms of payload capacity and engine power. A hypothetical hybrid-electric variant of each vehicle is analysed in combination with hypothetical HEL systems. Payload is given in Table 1.

Table 1: Platform payload for HEL system integration.

Parameter	Foxhound LPPV	Boxer MIV
Gross Vehicle Weight max. (kg)	7,500	38,500
Payload capacity (kg)	2,000	15,000

[17],[18],[19],[24]

3. HEL SYSTEM: CLASSIFICATION AND CHARACTERISATION

3.1. HEL Technology

There are three types of DEW; high-power microwave (HPM) / radio frequency DEW (RFDEW), millimetre-wave active denial (ADS), and high-energy laser (HEL), each with different electrical power requirements.

High-Power Microwave (HPM), Radio Frequency DEW (RFDEW) and Millimetre-Wave Active Denial Systems (MMW-ADS)

HPM and RFDEW systems operate at high peak power but low average power, because pulse widths of microseconds to milliseconds at typical repetition rates yield average electrical demands that are containable within standard vehicle alternator capacity

[27],[28]. The US Office of Naval Research identifies 'modest electrical power from the host platform' as a defining characteristic of HPM systems [9]. MMW-ADS are non-lethal area-denial weapons with no role in C-UAS (Counter-Unmanned Aerial System) or C-RAM (Counter-Rocket, Artillery and Mortar) missions, also with low power requirements. These systems do not present a powertrain architecture challenge, so they are not discussed further in this paper.

High-Energy Laser (HEL) Systems

Figure 1 shows a HEL system mounted on a Stryker 8x8 vehicle. HEL systems generate the output beam by using electrical power to generate photons via a pump diode array, driving a fibre laser or solid-state gain medium. The waste heat (60 to 70 per cent of input power) must be absorbed in the short term by thermal inertia and phase change material (PCM), requiring dedicated mass, and then rejected by a cooling system, which both adds weight and consumes power. [29], [30], [1] The cooling system must keep the HEL components at a temperature close to ambient and reject heat to ambient also, which for military equipment is specified up to 49 deg C atmospheric temperature, so chiller equipment is required. The load occurs in bursts of several seconds, punctuated by short re-engagement intervals and longer thermal recovery periods.

Ytterbium-doped fibre laser with spectral beam combining (SBC) is the dominant architecture for operationally fielded vehicle-mounted HEL systems as of 2026; all reference systems in Table 2 except HELLADS use this architecture. Chemical and free-electron laser technologies are excluded from further analysis on grounds of logistical impracticality and low maturity respectively for ground vehicle integration [1]

The key vehicle-mounted HEL systems that have been demonstrated are listed in Table 2.

Figure 1: *Directed Energy Maneuver Short-Range Air Defense (DE M-SHORAD) 50 kW-class laser weapon system mounted on a Stryker A1 8×8 armored vehicle. The roof-mounted beam director turret, internal laser and power-thermal management system (PTMS), and Ku-band AESA (Active Electronically Scanned Array) radar are visible.* ***Source:*** *U.S. Army Rapid Capabilities and Critical Technologies Office (RCCTO), image via Defense Visual Information Distribution Service (DVIDS). Public domain.*

Table 2: Summary of reference HEL systems. All data from open published sources. HELIOS is a shipboard system cited as an existence proof for 60 kW-class capability. Range figures are for hard-kill engagements against UAS targets where reported in open sources; n/r = not reported.

System	Platform	Output (kW)	Range	Ref
Raytheon HELWS	Wolfhound 6×6 (UK); JLTV (US)	15	~3 km	[6],[7]
US Army E-HEL	JLTV (US Army, future programme)	10–20	req. 4 km	[63]
AeroVironment AMP-HEL / LOCUST	JLTV (US Army)	20	n/r	[31]
Rheinmetall Skyranger 30 HEL	Boxer 8×8 (Bundeswehr); Pandur EVO (Austrian Army)	20 / 50 target	n/r	[26]
Lockheed Martin ATHENA	Ground demonstrator (US)	30	n/r	[32]
India DRDO Mk-II(A)	Ground mobile (India)	30	~3.5 km	[64]

System	Platform	Output (kW)	Range	Ref
Raytheon / Kord DE M-SHORAD (Guardian)	Stryker A1 8×8 (US Army)	50	n/r	[11],[33], [1]
Lockheed Martin HELIOS Mk 5 Mod 0	Maritime; USS Preble DDG-88 (USN)	60	n/r	[34],[35]
UK DragonFire	Land / Royal Navy (UK)	~100	~1 km	[2],[7]
Dynetics / Leidos HEL-TVD	FMTV M1083 6×6 truck (US Army)	100	n/r	[11]
DARPA HELLADS / General Atomics	Aircraft (MQ-9 class)	150	n/r	[36],[37]
US Army IFPC-HEL / Valkyrie	Semi-fixed site	>250	n/r	[11]

3.2. HEL Subsystem Architecture

The open-standard module taxonomy (classification of subsystems) for HEL systems is defined in the Directed Energy Weapon Systems (DEWS) Modular Open Systems Approach (MOSA) Reference Architecture, released by the US Department of Defense in July 2022 and developed by MITRE under contract to the Office of the Under Secretary of Defense for Research and Engineering (OUSD(R&E)). [38]. This taxonomy is shown in Appendix Table A1.

Four HEL modules dominate the electrical power requirement: the DE Source (the primary consumer), the Thermal Management Subsystem (PTMS), the Beam Director and the Power Conditioning and Storage Module.

Thermal Management

The PTMS is the heaviest subsystem for ground-based HEL systems, and consumes the most power. At current wall-plug efficiencies, 60% to 70% of the laser input power is rejected as waste heat during each engagement. Ground vehicles cannot exploit the ram-air cooling and low temperature air available to aircraft, so the PTMS must actively store and reject this heat through a liquid cooling loop and heat exchanger, augmented by phase-change thermal storage materials for burst absorption. [39] The mass of the PTMS depends on waste heat rejected, which depends on Wall Plug Efficiency (WPE), the ratio of the output power of the laser beam to the electrical power required to run the HEL system during firing. WPE values exceeding 50% have been reported under lab conditions, but if PTMS and other parts of a fully installed mobile system are included, then the reported values are much lower, around 35%.

3.3. Performance Classification: HEL Classes A–E

No standard taxonomy of HEL weapon classes by output power and target type exists in publicly available literature, beyond informal references such as “the 50 kW class”. The classification proposed here is derived in three stages. First, the fluence-to-kill thresholds that characterise each target category are taken from Zohuri [40] and tabulated in Appendix Tables A6 and A7, together with the progressive energy loss from atmospheric absorption, beam quality, and target surface reflectance. Second, these thresholds are compared against open-source programme evidence, comprising the known output powers of systems that have been physically demonstrated to defeat each target type. Third, class boundaries are drawn at qualitative steps in capability, i.e. power levels at which new categories of target become defeatable.

The five-class framework is summarised in Table 3; the programme references and defeat mechanisms for each class are given there. The derivation for each step is given in Appendix Tables A5–A7.

Ground vehicle engagement scenarios are assumed to be at or below the output power of Class E (500 kW). The primary target class requiring power substantially above this level is ballistic missile boost-phase intercept, with standoff ranges of 300–500 km, accessible only to airborne or space-based platforms [40, 11], and is therefore outside the scope of vehicle-mounted systems, regardless of available power. No ground vehicle engagement scenario identified in the open literature requires laser output exceeding 500 kW. Therefore if available vehicle platforms can support HELs up to Class E, then that is all that is required of ground -based systems.

Table 3: HEL Performance Classification: Classes A–E.

Class	Output Power (kW)	Primary Target Set	Defeat Mechanism
A	**20**	Optical sensors / IR seekers; Group 1–2 UAS (Unmanned Aerial System; quadcopters, FPV (First-Person View) drones, loitering munitions)	Photonic overload of detector array (sensors); composite avionics / airframe charring (UAS)
B	**60**	Group 3 UAS; one-way attack drones (Shahed-136 class); mortar rounds (81–120 mm) in flight	Composite structural failure by delamination or burn-through (UAS). Steel body heating and propellant / explosive ignition (mortar).
C	**150**	122 mm rockets; unprotected cruise missiles; fuel system ignition on armoured vehicles	Steel body structural defeat; propellant / fuel ignition; sustained ablation of light armour
D	**300**	Hardened RAM; cruise missiles with ablative coatings; rotary-wing aircraft	Sustained ablation through surface countermeasure; rotary-wing structural kill via rotor head and fuel system aimpoints
E	**500**	Manned fixed-wing aircraft; supersonic cruise missiles with heavy ablative coatings.	Deep structural kill by sustained ablation through thick metal skin at extended dwell times (~20–30 s); fuel system and control surfaces as preferred aimpoints. Ballistic missile boost-phase intercept is excluded, as it is not accessible from a ground vehicle.

3.4. HEL Efficiency and Specific Mass

3.4.1 WPE

Role of Efficiency. Wall-plug efficiency (WPE) governs both the electrical power for a given laser output when firing, and the associated power consumed by the PTMS and other HEL subsystems. A higher WPE reduces the installed mass as well as the power demand of the HEL.

Laser-Only versus Installed Efficiency. Laboratory measurements typically meter only the laser head and pump diode supply; chiller, compressors, pumps, and heat exchangers draw from a separate circuit [39], along with computer controls and other supporting subsystems, and are excluded. In a military vehicle installation all loads draw from the same bus, so installed WPE equals optical output divided by the combined demand of laser supply and all supporting systems. This boundary difference explains why field values of approximately 30–33% lie substantially below laboratory peaks of 50–56%. Full data sources are given in Appendix Table A2.

Reported WPE data. Seven data points are compiled in Appendix Table A2 and plotted in Figure 2. Gapontsev et al. (IPG Photonics, 2016) [41] demonstrated 51.2% WPE from a 10 kW Yb:fibre system under laboratory conditions — the highest confirmed published value for a coherent fibre laser at this power class in the open literature. Lockheed Martin reported a spectral-beam-combined fibre laser delivering 60 kW at WPE exceeding 43% [42], confirming that high laser-chain efficiency is maintained at elevated power. Current state-of-the-art is reported by Witte et al. (2025) [43] at 49–51% for fibre-coupled systems and 56% for free-space direct diode at 12 kW. The installed equivalent is approximately 33%, implied by a 2019 US Navy report [44] of a

450 kW electrical draw for 150 kW optical output from a shipboard system, consistent with field-condition estimates for military ground systems [44], [1].

No improvement trend is apparent in the installed data over time. The three installed data points available are from 2019 to 2025 and the values are from 33–35%. The laser-only data improves from 30% in 2011 to 51.2% in 2015, but after 2015 no improvement trend can be seen. Efforts to improve WPE should be expected as HEL's are adopted for military use, but the publicly available data gives insufficient basis for predicting a glide path for improvement.

3.4.2 Specific Mass

Specific mass data and adopted values. Figure 3 plots the reported open-source specific mass values for high-power laser systems against year. The two aircraft data points — Excalibur (DARPA/MQ-9, ~24 kW, ~5.0 kg/kW, 2013 [45]) and the HELLADS Laser Weapon Module (DARPA/General Atomics, 150 kW, ~4.0–5.0 kg/kW, 2015 [46]) — are laser subsystem figures only, presumably with ram-air cooling at altitude (cooler air) and no PTMS mass attributed. The RELI/Lockheed Martin figure (60 kW, ~5.0 kg/kW, 2017 [42]) is a ground-delivered system; it seems very likely that cooling equipment is not included. No discernible improvement trend is present across the four points, which span 2013 to 2017 and are between 4.0 and 5.0 kg/kW regardless of year or power class. Once fibre spectral-beam-combining was established as the dominant architecture, the laser source subsystem apparently did not continue to become lighter. A laser source specific mass of 4–5 kg/kW is therefore adopted as a fixed baseline.

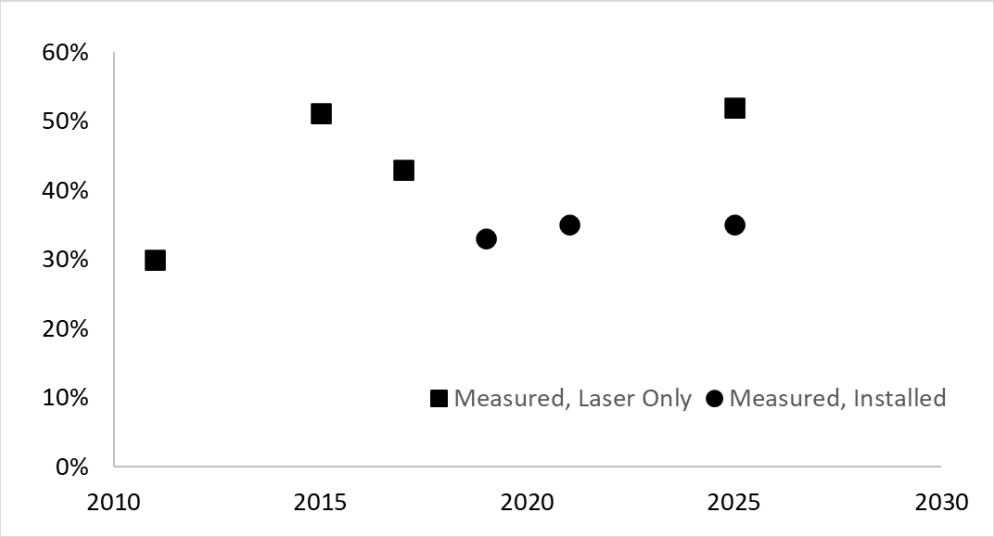

Figure 2: Wall Plug Efficiency (output power / input power)

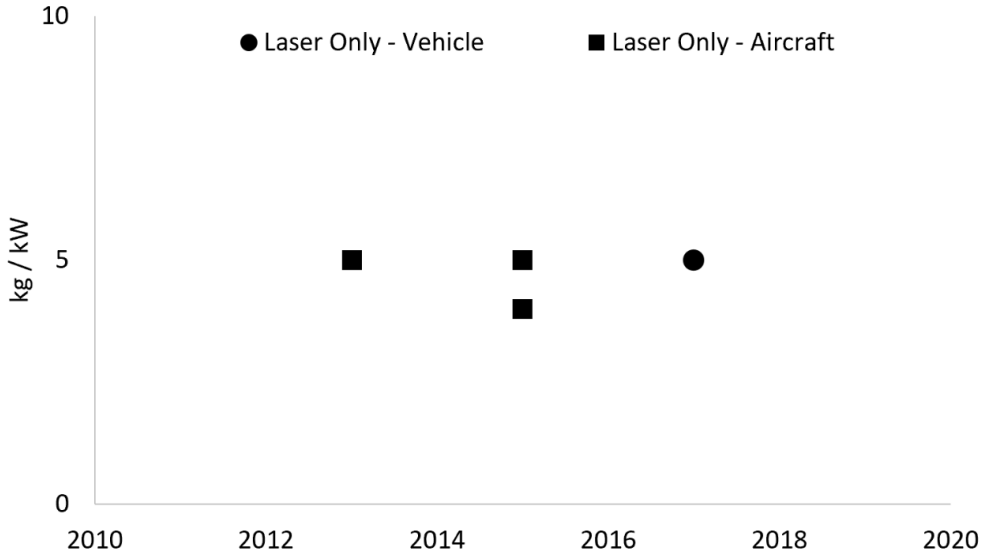

Figure 3: HEL Specific Weight (kg/kW)

3.5. Engagement Cycle Definition

A HEL system operates in a repeating three-phase engagement cycle:

• Engagement phase: Laser fires at target. A high power peak is drawn, and the laser output power during firing is the nominal output power describing the system. The required duration depends on target type, range, atmospheric conditions and laser power class, and presumably continues until the intended damage is visually confirmed, so is variable from shot to shot. Publicly reported test engagements range from seconds to tens of seconds.

• Re-acquire phase: Beam director slews to next target.

• Thermal recovery phase: PTMS dissipates accumulated waste heat. Engagement operations are suspended or severely rate-limited during this phase.

The large-capacity generator and battery of a hybrid powertrain, if already sized for Silent Watch and Silent Mobility functions, are well suited to the task of powering a HEL. They also provide a stable DC (direct current) voltage source that may enable simplification and weight reduction in the laser driver electronics.

The weapon system is characterised by the following inputs, for simulation purposes: the SFF (sustainable firing fraction, %, defined in section 1), the output power of the laser (kW), the wall plug efficiency (WPE, %) and the HEL system weight (kg). Given these inputs, it is possible to check through analysis that the generator, engine, inverter and battery are sufficiently sized so that the firing rate is never constrained by a lack of electrical power, and that the weight of the HEL and the weight of the hybrid powertrain do not exceed the weight capacity of the vehicle. Rapid screening software (ePOP Concept) is used for this purpose, first imposing the HEL electrical draw onto the stationary part of the Central European Mission Profile – Hybrid (CEMP-H) cycle, and then using the software to size the powertrain components to cover both the cycle requirements (including Silent Watch and Silent Mobility), and the engagement of the HEL while the vehicle is stationary. Both engine-running and engine-off (silent) modes can be considered for the engagement phase.

3.6. Estimation of Sustained Firing Fraction

The SFF (sustained firing fraction) is the fraction of total engagement cycle time during which the laser is firing. It is determined by the thermal recovery characteristics of the HEL. As these characteristics are not available in open sources for any fielded vehicle HEL system, the analysis adopts two bounding values of SFF rather than computing it from a specific t_rec assumption.

Upper bound: SFF = 83 per cent. Derivation: DragonFire field test data from the UK MoD reports defeat of a target travelling at 650 km/h with a dwell time of approximately 10 seconds [2][7]. CRS Report R46925 [11] states that beam director slew time between targets is of the order of several seconds; 2 seconds is adopted as a representative lower bound on slew time. Setting thermal recovery time to zero, the physical ceiling, achievable only if the PTMS can reject waste heat as fast as it is generated, gives SFF = 10 / (10 + 2) = 83 per cent.

Adopted value: SFF = 50 per cent. No open-source value for t_rec has been identified for any fielded system. SFF = 50 per cent is adopted as the single working assumption on tactical utility grounds: a weapon system that spends more than half its engagement cycle time in thermal recovery seems unlikely to maintain a useful engagement rate against a sustained aerial threat. SFF = 50 per cent is therefore treated as the practical floor for a tactically effective system. This approach avoids speculating on PTMS recovery performance, which varies with power class, ambient temperature, and cooling architecture, none of which are quantified in open sources for any fielded system. The value of SFF may be adjusted when the methodology of this paper is applied, so an error in the selected value would not invalidate the analysis method.

3.7. Smoothing the Power Demand Peaks with Ultracapacitors

The power demand of the HEL is illustrated in Figure 4, for a HEL of class A. A standby load is replaced by alternating loads for firing and recovery. The pattern repeats every few seconds. The large battery of a hybrid powertrain may be considered suitable for accommodating the demand peaks, but in practice this might force an even larger battery size, simply because charging rate should be limited in order to preserve the durability of the battery. Ultracapacitors offer a much cheaper and lighter solution. By comparison with batteries, they lack energy density (kWh/kg) but excel in power density (kW/kg). The frequency of alternation is suitable for the use of ultracapacitors to smooth out the power demand to an average value during operation. For example, a commercially available ultracapacitor module from Skeleton Technologies is advertised with power capacity 504 kW and energy capacity 225 Wh, and it weighs 35 kg. [47] If such ultracapacitors are used to smooth out the power draw for a Class A HEL, as illustrated in Figure 4, the charging and discharging power would be approximately 24 kW for 3 seconds, with a total energy storage of 20 Wh. For a class E HEL, the values would be approximately 500 kW for 15 seconds, giving 417 Wh, containable with two ultracapacitor modules weighing only 70 kg, a negligible added weight by comparison with the payloads of the two vehicles. Ultracapacitors work between a wider range of voltages than batteries, so a DC-DC (DCDC) converter is also required. A HEL system is assumed to use ultracapacitors, so that the vehicle need supply only the average power required during engagement, not the peak.

3.8. Electrical Power Demand

The total vehicle electrical demand is the sum of five component groups, listed in Table 4. Three of these — the laser chain, the chiller, and the coolant pumps — scale with laser output power and dominate at all but the lowest power class. Two are fixed regardless of laser power class: the beam director drive load (which scales weakly with aperture size) and the fixed loads (acquisition, tracking, and pointing sensors, fire control computer, and communications). Appendix Table

A3 defines each component's behaviour, worked example values, and the assumptions underlying the model.

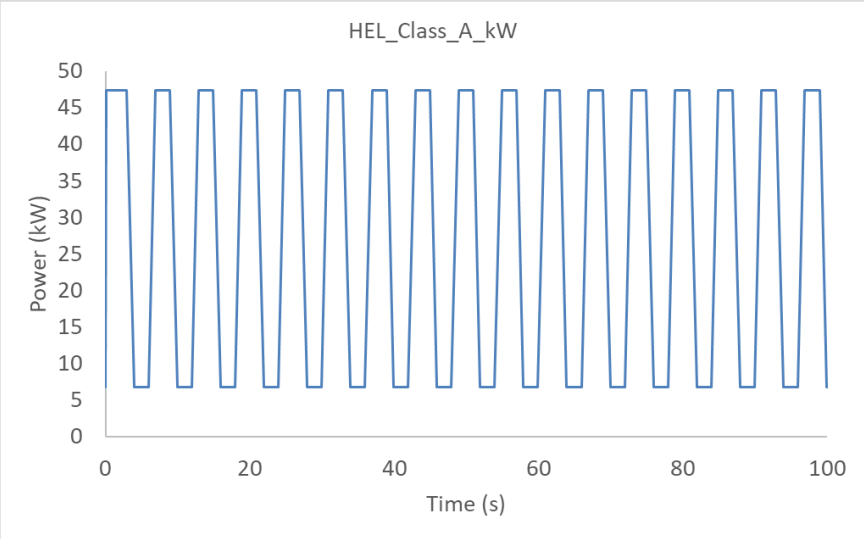

Figure 4: Power demand for HEL system. Standby mode followed by alternating firing and thermal recovery, for SFF = 50%. This power demand can be smoothed to near-constant average values by the use of ultracapacitors.

Table 4: DEW subsystem specific mass at 100 kW output. Further details in Appendix Table A9.

Subsystem	kg/kW (low)	kg/kW (high)
DE Source (laser, pump diodes, SBC combiner, output optics to BD aperture)	4.4	5.0
Thermal Management / PTMS (liquid loop, pump, HX, PCM, vehicle-side HX)	2.0	2.8
Beam Director (steerable telescope, gimbal, ruggedised MIL-STD-810)	2.0	4.0
ATP (Acquisition, Tracking and Pointing) Sensors (EO/IR tracker, radar cue receiver, processor)	0.5	1.5
Platform Integration (mounts, EMI (Electromagnetic Interference) shielding, harness, connectors, armoured housing)	0.5	1.5
EPS (Electrical Power System) / Power Conditioning (DC-DC converter, EMI filter, isolation transformer)	0.5	1.0
Fire Control and Track Manager (ruggedised processor and I/O)	0.2	0.5
Beam Transport (internal fibre, DE Source to BD aperture)	0.1	0.2
TOTAL	**10.2**	**16.5**

Chiller Coefficient of Performance

The chiller is assumed to be a conventional vapour-compression refrigeration system that removes waste heat from the laser's optical components and rejects it to the ambient air. Its electrical demand is determined by the quantity of waste heat to be removed and the chiller's coefficient of performance (COP) — the ratio of heat removed to electrical work input. A higher COP means the chiller draws less electrical power for a given cooling load.

COP is governed by the temperatures of the heat source (the laser coolant) and the heat sink (the ambient air). The theoretical upper limit — the Carnot COP — is set by these temperatures alone, and is derived from the second law of thermodynamics (see, for example, Cengel and Boles, Thermodynamics: An Engineering Approach, McGraw-Hill, current edition, Chapter 6). Real chillers achieve a fraction of the Carnot limit depending on compressor efficiency and refrigerant properties. Table 5 derives the adopted COP value step by step.

Parameter	Value	Derivation and basis
Laser coolant return temperature (heat source, T_cold)	**20°C**	Representative inlet temperature for a fibre laser diode coolant loop.
Heat rejection temperature (T_hot)	**60°C**	MIL-STD-810G, Method 501.7.
Theoretical maximum COP (Carnot COP)	**7.33**	Calculated from T_cold and T_hot.
Practical efficiency fraction (real / Carnot)	**51%**	Consistent with published data for scroll and reciprocating compressor systems.
Adopted COP	**3.7**	COP = 51% of Carnot COP = 0.51 × 7.33 = 3.74

Table 5: Derivation of the adopted chiller COP. Further details in Appendix Table A7.

The adopted COP of 3.7 is cross-validated against published data for analogous vapour-compression systems operating at a similar temperature lift. Automotive R-134a refrigerant circuits, condensing at 45 to 50°C and evaporating at approximately 5°C (a temperature lift of 40–45 K), achieve COP values of 2.4 to 3.6 under hot-ambient test conditions. The NIST benchmark for R-134a cycles gives COP of approximately 3.0 to 3.5 at 32°C ambient [49][50]. The DEW PTMS evaporating temperature of 20°C is warmer than in both automotive cases, which reduces the pressure ratio across the compressor and raises the attainable COP above the automotive range. Yang et al. [51] report a 15 kW(thermal) aircraft galley cooling unit with an evaporating temperature of −9°C — a harder thermodynamic duty than the DEW case — with a system mass of 83 kg (5.5 kg per kW(thermal)); the implied COP is consistent with the sub-zero evaporating temperature. The adopted COP of 3.7 sits at the upper end of the automotive experimental range and is consistent with the temperature-lift advantage of the DEW application relative to standard automotive air-conditioning duty. It is presented as an engineering estimate; no open-source military chiller test data at this temperature lift and capacity has been identified.

Firing and Non-Firing Phase Demands

During the firing phase, the dominant loads are the laser and the chiller. During the non-firing phase (beam director slewing between targets, or thermal recovery), the laser is off but the chiller continues to run at full load to discharge the phase-change material (PCM) thermal store that absorbed the burst waste heat.

The average vehicle electrical demand is the weighted sum of the firing-phase and non-firing-phase demands, weighted by the SFF and smoothed by ultracapacitors, as described in Section 3.7.

Installed System WPE and Numerical Results

The installed system wall-plug efficiency is the ratio of average laser output to average vehicle bus demand, integrated over the full engagement cycle. It is always substantially lower than the laser-only WPE of 50 per cent, because the chiller and fixed loads draw power throughout the cycle while the laser produces output only during the firing phase. At low power classes the fixed loads are significant; at Class C and above the chiller dominates, and the system WPE converges to a stable value determined by thermodynamic analysis.

Table 6 gives numerical results for all DEW classes at SFF = 50%. All values are computed from the component model and the COP derivation in Table 5.

Class	Laser output (kW)	Firing-phase demand (kW)	Average demand at SFF=50% (kW)	System WPE at SFF=50% (%)
A	20	48	27	36.8%
B	60	134	73	41.2%
C	150	328	176	42.5%
D	300	652	348	43.1%
E	500	1,084	579	43.2%

Table 6: Electrical Power Demand and System WPE by HEL Class

Model parameters: Laser-only WPE = 50% throughout (Gapontsev et al. [41]). Chiller COP = 3.7 (Table 5). Fixed loads = 3.5 kW. Beam director: 2.0 kW active at Class B, scaling sub-linearly with power class; 0.5 kW idle (non-firing). Coolant pumps = 3% of chiller electrical draw. Chiller runs continuously at rate P/COP throughout firing and non-firing phases (cycle-average model). Non-firing demand = chiller + beam director idle + fixed loads. System WPE = (SFF × laser output) / average bus demand over full engagement cycle; always lower than laser-only WPE because chiller and fixed loads draw power throughout.

3.9. Chiller Specific Mass

The PTMS comprises several heavy components: the vapour-compression refrigeration circuit (compressor, condenser coil, expansion valve, and evaporator at the laser head), a phase-change material (PCM) thermal store that absorbs burst waste heat during the engagement phase, liquid coolant circuit plumbing and manifolds, condenser fans or liquid-to-air heat exchangers, and an electronic controller. This sub-section derives the chiller circuit contribution, which is the component directly sized by the COP analysis above.

Chiller thermal capacity sizing

The chiller must reject the average waste heat over the full engagement cycle. The PCM thermal store absorbs burst waste heat during firing; the chiller then operates during the non-firing thermal recovery phase to drain the store. The required chiller thermal capacity is therefore not the instantaneous peak waste heat rate but the cycle-average rejection rate. For a laser of output power P at wall-plug efficiency WPE, the required average chiller thermal capacity is:

$$Q_{chiller} = P \times SFF \times (1 - WPE) / WPE \quad (1)$$

Commercial reference data for chiller specific mass

No open-source specific mass figure has been identified for a military DEW PTMS refrigeration circuit at this capacity and operating temperature. Three commercial reference points are used to bound the estimate. All three operate at a temperature lift of approximately 40 K, matching the DEW case.

(a) **Aircraft galley cooling unit (Boeing 787 application):** Yang et al. [51] report a 15 kW(thermal) unit with a system mass of 83 kg, giving 5.5 kg per kW(thermal). The evaporating temperature is −9°C, a harder duty than the DEW case (20°C), and the unit is qualified for aircraft use with associated structural and reliability requirements. The 5.5 kg per kW(thermal) figure is therefore treated as an upper bound for equivalent thermal capacity at DEW PTMS duty.

(b) **Automotive vapour-compression circuit (R-134a, 3–5 kW capacity, engine-driven compressor, condenser, evaporator, and refrigerant charge, excluding housing and controls):** Product data for the Sanden SD7H15 compressor (8.0 kg assembly, capacity approximately 7.6 kW(thermal)) [52] and the Classic Retrofit Electrocooler (complete circuit under 15 kg for similar capacity) [53] give a derived specific mass of approximately 3 to 5 kg per kW(thermal). These are commercial components without military qualification margins; a 20 to 30 per cent uplift for militarisation gives 4 to 6 kg per kW(thermal).

(c) **Bus rooftop air-conditioning unit (Thermo King Athenia AM II 1000, 26–31 kW(thermal) capacity, 213 kg complete integrated unit including structural housing, condenser fans, and controls)** [54]: Total specific mass is 7 to 8 kg per kW(thermal). The housing, fans, and structure account for a substantial fraction; the refrigeration circuit alone is estimated at 4 to 5 kg per kW(thermal) by comparison with Mobile Climate Control Reference Manual evaporator unit data [55], which gives 27 kg for an 8 kW(thermal) evaporator section and 43 kg for a 14 kW(thermal) unit at ARI test conditions (3.4 and 3.1 kg per kW(thermal) for the evaporator section).

Adopted range and conversion to kg/kW

Across these three reference points, the refrigeration circuit alone falls in the range 4 to 5.5 kg per kW(thermal), with the aircraft figure as the upper bound and the automotive figure as the lower bound. This range is adopted as an engineering estimate.

The PTMS becomes heavier for the higher value of SFF because the average waste heat increases. However, this is assuming that the system is sized for the worst case of 49 deg C ambient temperature, which in practice is very rare. A practical design solution might target full function at lower temperatures, with de-rating of SFF above a selected temperature.

3.10. Installed System Mass by Class

Table 7 gives the resulting specific mass range and total installed mass range for each HEL class. The values are plotted in Figure 5.

Class	Laser output (kW)	Average Power Draw, During Engagement (kW)	Total installed mass range (kg)
A	20	27	358–580
B	60	73	732–1,184
C	150	177	1,328–2,149
D	300	349	2,083–3,374
E	500	578	2,900 – 4,700

Table 7: Estimated installed HEL system mass range by class.

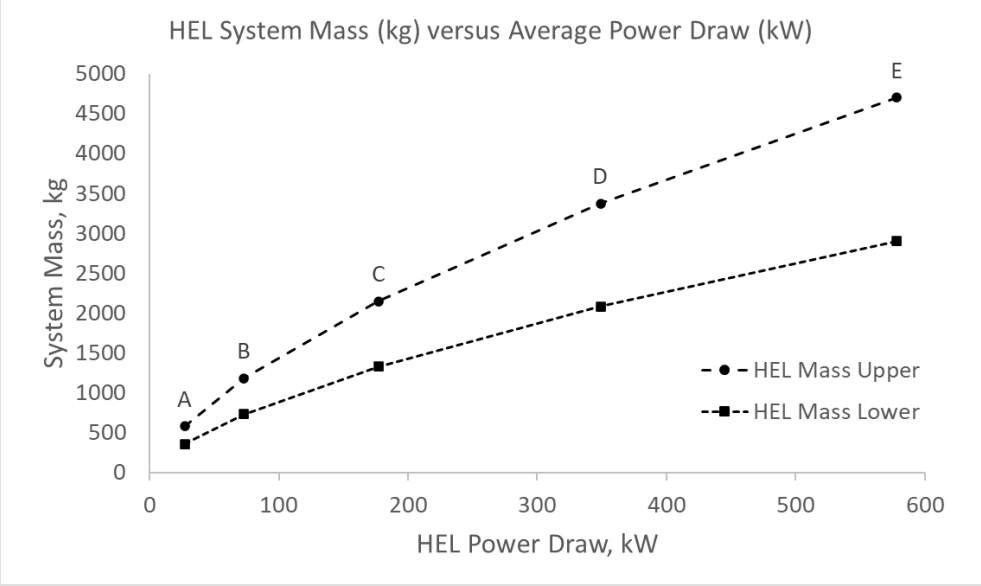

Figure 5: HEL System Mass (kg) versus Operational Power Draw (kW).

The mass table and the electrical demand table together define the two constraints that a candidate hybrid powertrain must satisfy simultaneously. The powertrain addition must remain within the platform payload budget after the HEL system mass is allocated. The powertrain's engine, generator and inverter must be capable of sustaining the average electrical demand at the selected SFF, or of providing sufficient power so that the battery can sustain HEL engagement for the required duration, if time-limited operation is allowed.

4. ANALYSIS METHODOLOGY

4.1. Mission Profile CEMP-H combined with HEL Power Draw

The land-based mobile HEL of the future will probably be mounted on tactical wheeled vehicle platforms that are also required to provide Silent Watch, Silent Mobility and Export Power. Such vehicles are presumed to have hybrid powertrains, as ICE-only powertrains cannot deliver these functions without additional generators, and BEV powertrains cannot operate without charging stations. A Mission Profile CEMP-H for powertrain analysis of hybrid tactical wheeled vehicles is proposed in [56].

The CEMP-H is a 24-hour mission cycle comprising nine phases, designed to include all powertrain modes required of a hybrid tactical wheeled vehicle. The phases include road and cross-country transit, a five-hour Silent Watch period (engine off, stationary), a two-hour Silent Mobility patrol (engine off, 20 km/h), a one-hour stationary phase for weapons engagement (engine on, full electrical load), and a base rest period that includes both engine-on Export Power and engine-off fractional Export Power. The cycle is defined as charge-neutral over 24 hours: restoration of the initial state of charge must be demonstrated within the simulation, not assumed. Vehicle-specific calibration parameters — gross vehicle mass, road load coefficients, maximum speed, auxiliary electrical load, and Export Power — are given for both platforms in [56, Tables 2 and 3].

The companion paper [56] analyses the CEMP-H cycle for both Foxhound and Boxer without a HEL load, and sizes series and parallel hybrid powertrains for each. The series hybrid architectures from that analysis form the starting baseline for this paper. The engagement phase of the CEMP-H — the one-hour stationary period with the engine running — is the appropriate phase for the addition of the HEL electrical load, on top of the continuous auxiliary load already present. The engine, generator and rectifier hardware is sufficient to support burst-energy delivery to the HEL, supplemented by the ultracapacitors described in Section 3.7, with upgrades required only for the highest class HEL on each platform (class C for Foxhound and class E for Boxer). The series hybrid powertrain specifications from [56] are shown in the Series Hybrid baseline columns of Tables 8 and 9.

This paper considers adding HEL systems of classes A-E to each hybrid platform, and analyses the weight and power impacts in each case, re-specifying the powertrains where necessary to support the extra power of the HEL.

4.2. ePOP Concept Methodology

ePOP Concept (version 1.0, ZeBeyond Ltd, Leamington Spa, UK) is a rapid parametric powertrain screening tool that generates alternative vehicle powertrain architectures to cover a user-supplied load profile, provided as one or more parallel time-series of power (kW) versus time (s). The possible architectures include conventional ICE, battery-electric (BEV), and hybrid configurations. The software can analyse a wide range of vehicles including passenger cars, trucks, off-highway vehicles with hydraulic drives, and VTOL (Vertical Take-Off and Landing) aircraft. For the purposes of this paper, however, discussion is confined to the Foxhound

and Boxer platforms, with diesel-electric hybrid and conventional internal combustion engine (ICE) architectures, powered by JP-8 military diesel fuel.

The tool's methodology, component efficiency assumptions, and accuracy boundaries are described in [14] and assessed in the context of tactical vehicles in [56]. ePOP Concept applies fixed-efficiency and fixed-density models for each powertrain component, sizes each component to meet the peak and average demands of the load cycle, and outputs component specifications, mass, and estimated cost. A single model setup covers all architectures being compared without requiring separate model builds per configuration — an important advantage when screening multiple HEL power classes against multiple platforms simultaneously. The companion paper [56] provides the complete step-by-step procedure for setting up the CEMP-H cycle in ePOP Concept, together with the open-access Excel workbooks used to generate the power-time inputs; that procedure is not repeated here.

For this paper, the CEMP-H baseline power-time traces from [56] are used as the starting load. The average HEL power demand from Table 6, smoothed to a constant value by ultracapacitors per Section 3.7, is added as a further DC electrical load in the engagement phase. ePOP Concept then re-sizes the ICE, MGU, rectifier, inverter, DCDC converter, and battery to cover both the full CEMP-H cycle and the HEL engagement load, outputting the resulting powertrain mass and cost for each configuration. The series hybrid architecture is used throughout, rather than the parallel hybrid, because it completely decouples the engine operating point from the traction demand; for example, the engine can recharge the battery continuously at full power while moving, as the speed of the vehicle is controlled independently from the speed of the engine.

4.3. Architecture Configurations Evaluated

Table 7 gives the system mass for each HEL class. The corresponding HEL power demand is shown in Table 6, being the sustained average electrical power that the vehicle powertrain must supply, to support continuous HEL engagement. It is assumed that the HEL system will include ultracapacitors to level out the spikes in the power demand, requiring a very small mass of capacitors compared to the whole system, as described in Section 3.7. The ICE output, generator, inverter and battery capacity must therefore be sized such that the vehicle can sustain the average power delivery over the operational engagement period, while also meeting mobility requirements in different phases of the CEMP-H cycle. With the HEL mass and power demand defined, parallel-hybrid and series-hybrid powertrain configurations were evaluated for each platform.

5. RESULTS

Figure 6 shows the powertrain architecture for a parallel hybrid, generated by ePOP Concept, and Figure 7 shows a series hybrid. The bottom output in each diagram is the electrical supply to the HEL system. The series architecture was selected for both Foxhound and Boxer.

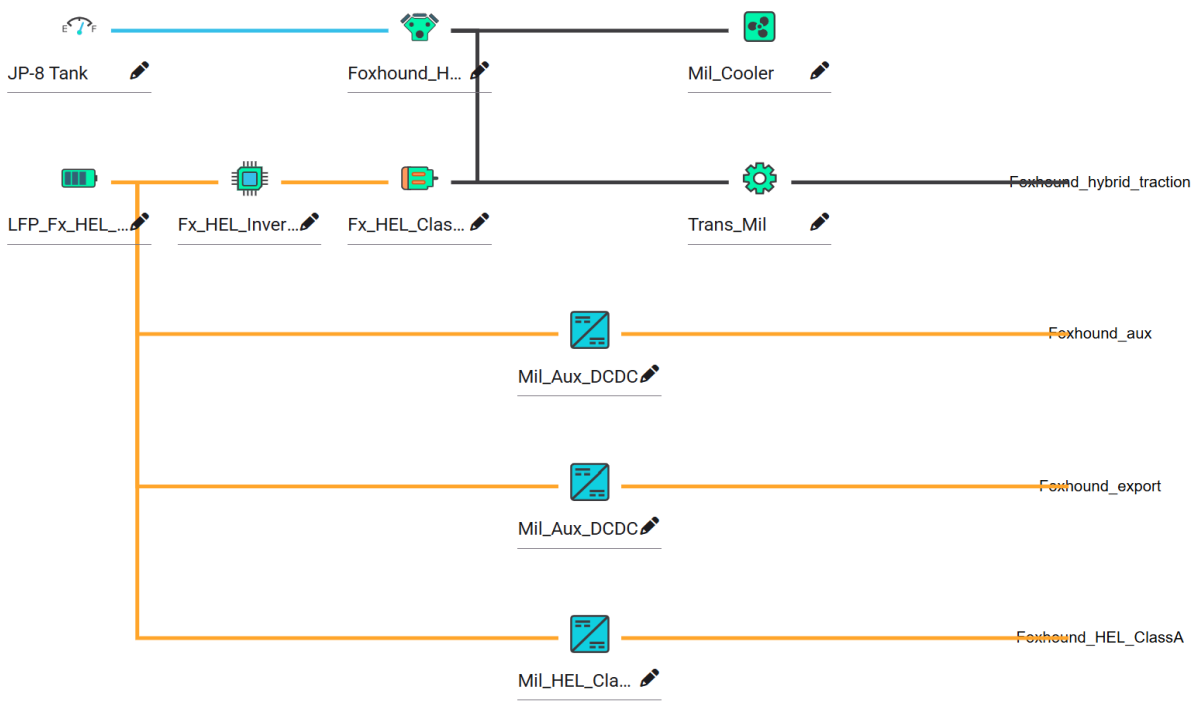

Figure 6: Parallel-Hybrid Architecture with HEL Power Output

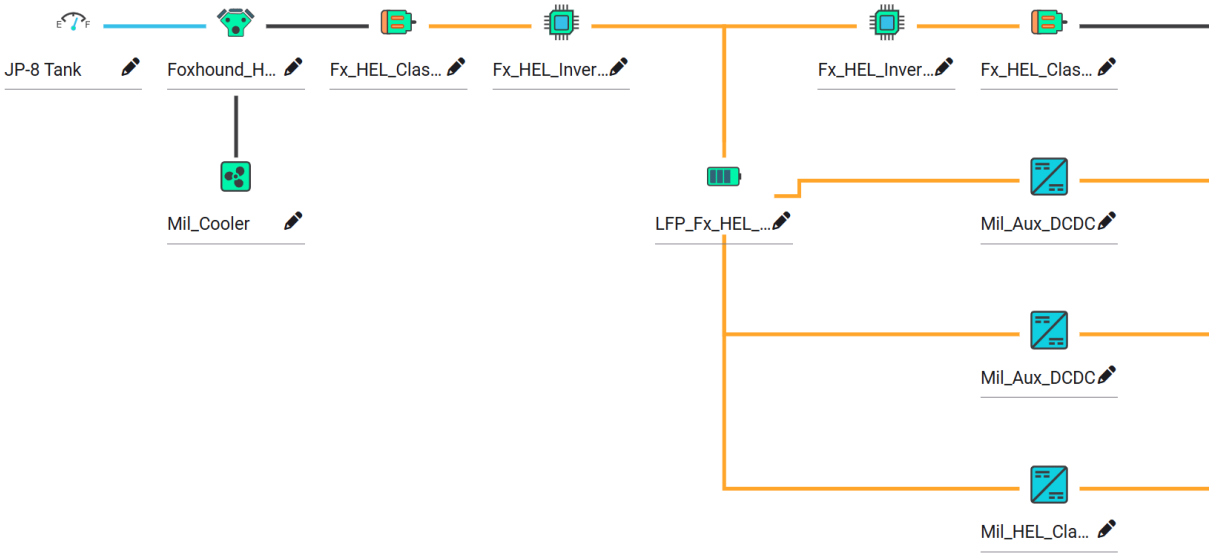

Figure 7: Series-Hybrid Architecture with HEL Power Output

		ICE Only	Parallel Hybrid	Series Hybrid	Series with HEL Class A	Series with HEL Class B	Series with HEL Class C
ICE	kW	160	160	160	160	165	228
MGU (Motor Generator Unit)	kW		152	152	152	152	203
Rectifier	kW			146	146	146	195
Inverter	kW		140	140	140	140	140
Motor + Gearing	kW			133	133	133	133
Transmission	kW		144				
DCDC Converter	kW		42	42	42	87	195
Battery	kWh		65	65	65	65	65
Fuel Tank mass	kg	244	222	252	253	252	252
Powertrain Mass	kg	781	1625	1907	1915	1922	2196
P/T Mass Added	kg			Base (0)	8	15	289
HEL mass (lower)	kg				358	732	1328
Payload	kg			2000	1634	1253	383

Table 8: ePOP Concept specifications and mass for Foxhound in ICE, hybrid and HEL configurations.

		ICE Only	Parallel Hybrid	Series Hybrid	Series with HEL Class C	Series with HEL Class D	Series with HEL Class E
ICE	kW	600	600	600	600	600	704
MGU	kW		570	570	570	570	669
Rectifier	kW			547	547	547	642
Inverter			525	525	525	525	525
Motor + Gearing	kW			499	499	499	499
Transmission	kW		542				
DCDC Converters	kW		83	83	205	385	623
Battery	kWh		210	210	210	210	210
Fuel Tank mass	kg	742	616	766	766	766	766
Powertrain Mass	kg	2679	5183	6604	6659	6719	7223
P/T Mass Added	kg			Base (0)	55	115	619
HEL mass (lower)	kg				1328	2083	2900
Payload	kg			15000	13617	12802	11482

Table 9: ePOP Concept specifications and mass for Boxer in ICE, hybrid and HEL configurations.

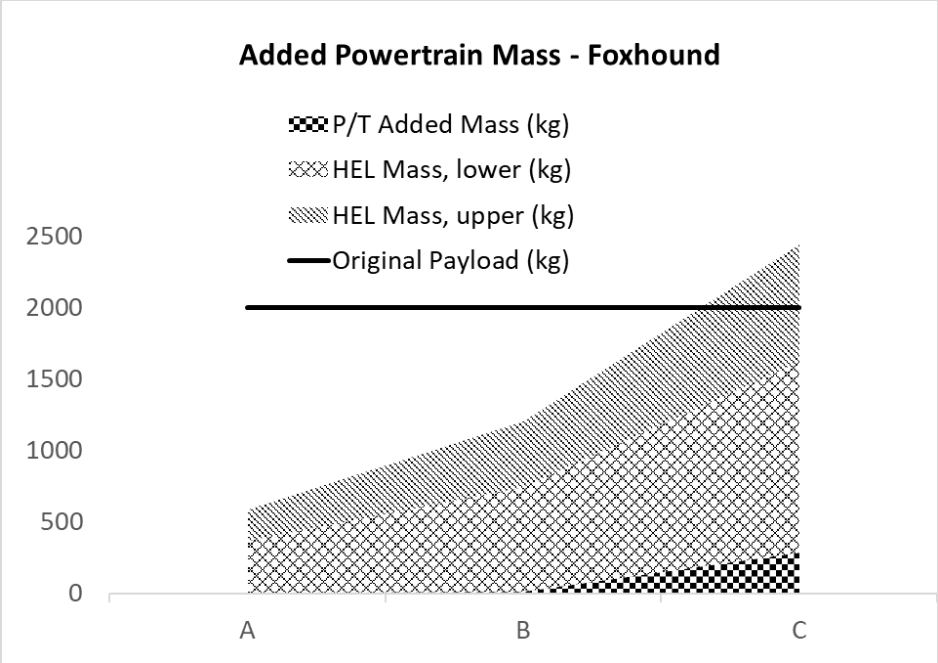

Figure 8: System Mass (kg) versus HEL Class – Foxhound

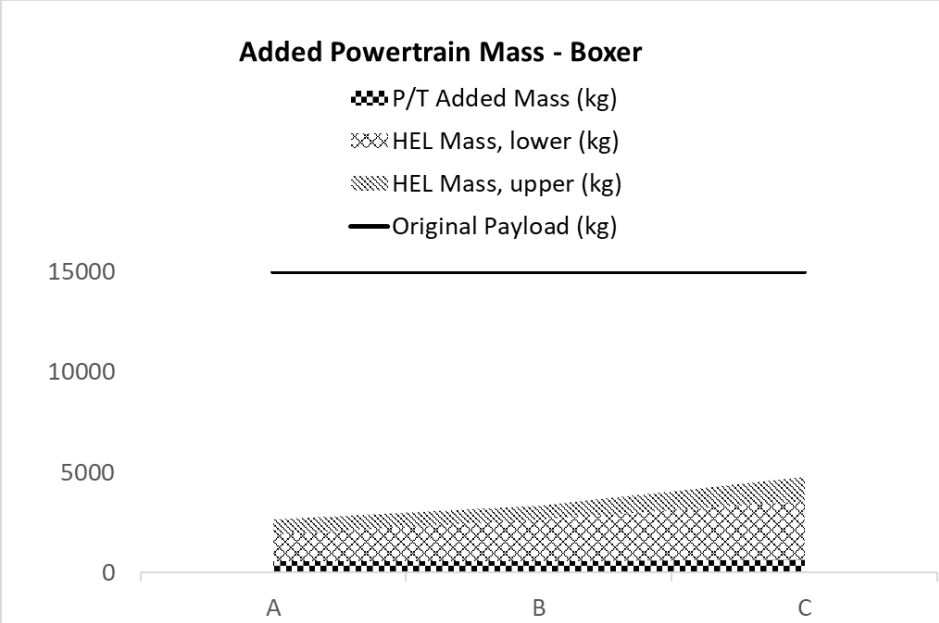

Figure 9: System Mass (kg) versus HEL Class - Boxer

Tables 8 and 9 show how the power specifications of the powertrains increase, along with the weight, as the vehicle is hybridised and HEL is added. Figures 8 and 9 illustrate the results. "Payload Remaining", in the tables, assumes the Series Hybrid is designed with weight savings to preserve 2,000 kg and 15,000 kg payload for the two vehicles, so that any weight addition for the HEL is taken out of these payloads. A minimum payload of 240 kg should remain, for a driver and a gunner: 120 kg is allowed per person, comprising 85 kg soldier body mass (95th percentile NATO male), 15 kg combat body armour, and 20 kg personal weapon, ammunition and equipment. This is an engineering estimate that is consistent with planning figures used in UK MoD vehicle procurement.

6. DISCUSSION

The chief obstacles to mounting a HEL on a vehicle platform are the power requirement and the system weight. Both are illustrated in Figure 5, for HEL classes A-E.

The Foxhound and Boxer hybrid powertrains proposed in [56] are already equipped to provide export power, via substantial generators and inverters sized for the requirements of the CEMP-H mission profile. Tables 8-9, and Figures 8-X2, show that the necessary enlargement of the Foxhound powertrain components for HEL is minimal for Class A-B, and likewise for Boxer with Class C-D. Only the highest classes for each vehicle (C and E) mandate significant powertrain upgrades, which are containable within the payload capacity of each vehicle. This holds for all cases except Foxhound with the Class C HEL, which is feasible only if the HEL system mass is closer to the lower estimate than to the higher.

The series hybrid platform offers a further advantage. A standalone vehicle HEL EPS must power the laser driver, typically requiring a dedicated diesel generator, AC bus, rectifier, and power conditioning unit. On a series hybrid platform, the traction battery and stabilised high-voltage DC bus are already present as standard features of the drivetrain. The HEL EPS therefore reduces to a single DC-DC converter and EMI filter, eliminating the AC front-end entirely. The EPS specific mass adopted in Table 4 is therefore 0.5–1.0 kg/kW rather than the 1.0–2.0 kg/kW typical of a standalone EPS. The saving scales with power class and is therefore most valuable for Classes C–E, where payload margin is most constrained. This synergy is one reason the series hybrid is the natural host architecture for a vehicle-mounted HEL, confirming that hybridisation for Silent Watch and Silent Mobility prepares the platform for HEL integration at relatively low incremental cost. (The batteries sized in [56] for Silent Watch and Silent Mobility (65 kWh for Foxhound, 210 kWh for Boxer) are also sufficient in both power and energy capacity to support HEL deployment for a limited time with the engine off, should that be useful, but this capability is not discussed further in this paper.)

The ICE power requirements for HEL Class C and Class E increase to 228 kW (Foxhound) and 704 kW (Boxer), both of which are obtainable with commercially available engines. If, however, engines of sufficient power cannot be obtained, several measures could reduce the requirement:

1. Reduce the SFF below 50%.
2. Reduce the size of the laser cooling system to provide full SFF at a lower ambient temperature than the assumed 49 deg C, and accept de-rating of SFF at higher temperatures.
3. Seek improved WPE from the laser system.
4. Reduce the target output power (150 kW, 500 kW) for Classes C and/or E.

The weight of the powertrain is already increased substantially with the first step (hybridisation) before HEL is added, as the system is sized to provide Silent Watch, Silent Mobility and Export Power, as explained in the companion paper. [56] For the addition of a HEL, the series hybrid is assumed as baseline rather than the parallel hybrid, despite being heavier, because the series hybrid

completely detaches the engine operating point from the demands of the HEL and the traction drive, so they can operate independently. The series-hybridisation step itself adds 1126 kg to the Foxhound per Table 8, but it is assumed that weight savings will be achieved elsewhere in the case of such a major redesign, deliberately preserving the original payload of 2,000 kg as a programme target, as is the usual practice with commercial vehicles. (The 7,500kg GVM of the Foxhound cannot be increased, as higher GVMs require a different driving licence for operators in Europe and the UK.)

The last rows of Tables 8-9 track the remaining payload as HEL hardware is added, with the series hybrid as baseline, and Figures 8-9 illustrate it.

Table 8 shows that the addition of a Class A or Class B HEL to the Foxhound vehicle has very little effect on the specifications of the hybrid powertrain, confirming the synergy of combining hybridisation with HEL. The step up to Class C almost doubles the required engine power, but this is containable with only a further 274 kg added to the powertrain weight.

The Boxer has a payload of 15,000 kg. Figure 9 shows that this is far more than required to accommodate even the Class E laser.

7. CONCLUSIONS

Matching a HEL system to a vehicle platform at concept stage is a multi-dimensional problem: power demand and installed mass both vary with HEL parameters that are unlikely to be frozen early in a program, and the power demand itself can trigger further mass increases in the powertrain additional to those of the hybridization step. The methodology presented here allows these interactions to be analyzed rapidly, and requires no specialist simulation expertise; ePOP Concept screens multiple HEL power classes against multiple platforms simultaneously, requiring only limited vehicle data that is readily available at concept stage.

Five HEL classes (A–E) are defined by target type and laser output up to 500 kW, covering the full range of land-based applications. Power demand and installed mass scale from Class A to E, and are compared with platform payloads. Applying ePOP Concept to the CEMP-H mission profile for Foxhound and Boxer shows that each platform can accommodate specific HEL classes within its payload and engine power envelope, with only Class C and E respectively requiring engine uprates.

The Foxhound platform in series hybrid form could support a HEL class A-B with very little modification to the powertrain, assuming that it was already specified to deliver Silent Watch and Silent Mobility functions according to the CEMP-H mission profile. Class C is also attainable if the engine power is increased. A Boxer series hybrid platform could support a HEL up to class D in respect of both weight and engine power, and even up to class E at 500 kW laser output, given an engine uprate to 704 kW.

Appendix A

Appendix Table A1: HEL weapon system functional modules.

DEWS MOSA RA Module	Function	Primary Mass Driver?	Primary Power Driver?	Ground Vehicle Notes
DE Source	Fibre laser or solid-state gain medium; generates the output beam by converting electrical pump energy to photons via stimulated emission	Moderate	High	
Thermal Management (PTMS)	Absorbs and rejects waste heat generated by DE Source at current WPE; phase-change material stores, liquid cooling loop rejects via heat exchanger	High	High	Cannot use ram-air cooling available to aircraft.
Beam Director	Steerable telescope assembly that focuses and aims the output beam; provides 360° or hemispherical azimuth coverage; closed-loop tracking during engagement	Moderate	Low	Roof- or turret-mounted on ground vehicles; must tolerate vehicle vibration and dust.
Beam Transport	Optical path (fibre or free-space) from DE Source to Beam Director; on ground vehicles typically a short internal fibre run reducing complexity relative to naval or aircraft installations	Low	Negligible	Fibre delivery simplifies vehicle integration relative to free-space transport; standard for modern fibre-laser designs
Power Conditioning and Storage	DC-DC converters, battery banks, and bus conditioning; provides burst energy for engagements from stored charge; recharged by vehicle generator between engagements or during thermal recovery	Moderate	Moderate	Battery sizing driven by engagement burst energy and minimum SOC (State of Charge) constraint; ultracapacitors are an alternative for short (<20 s) burst discharge with rapid recharge Ref: Khalil et al., SAE, 2017, [57]. Requirements may be partially provided by hybrid system.

DEWS MOSA RA Module	Function	Primary Mass Driver?	Primary Power Driver?	Ground Vehicle Notes
Fire Control	Engagement sequencing, aimpoint maintenance, lethality assessment, and safe-to-fire logic; interfaces with vehicle battle management system	Low	Low	Software-intensive; mass-negligible for vehicle integration purposes
Track Manager	Maintains mathematical representations (tracks) of objects of interest; associates detections from multiple sensors; provides track priority to Beam Director	Low	Low	Closely integrated with Integrated Sensors and Fire Control; distinction matters for MOSA compliance but not for mass/power analysis
Integrated Sensors (ATP)	Electro-optical and radar sensors for target acquisition, identification, and tracking; includes Ku-band AESA radar and EO/IR camera suite on current systems such as DE M-SHORAD [33]	Low	Moderate	Radar and EO/IR sensors add mass but are modest relative to PTMS; already present on air-defence vehicles as standard fit
Human Machine Interface (HMI) and Safety	Operator display, engagement authorisation, safety interlocks (beam inhibit if friendly in path), and interface to crew situational awareness systems	Low	Low	Mounted in crew compartment or mission module operator station
Host Platform Interface	Mechanical, electrical, data, and cooling interfaces between the HEL system and the host vehicle; in Boxer MIV this is the mission module electrical and data bus interface	Low	Low	Critical for integration planning; defines what the vehicle powertrain must supply (voltage, current rating, bus interface standard)

HEL weapon system functional modules per the DEWS MOSA Reference Architecture [38], with ground vehicle integration notes. 'Primary mass driver' and 'power consumer' classifications are the author's assessment for ground vehicle applications based on published programme data; see text for derivation.

Appendix Table A2: Wall Plug Efficiency: Plotted Data Points and Asymptotes

Year	Graph Series	WPE (%)	Description
2011	Measured, Installed	~30%	Early installed benchmark. Derived from pump diode and quantum defect physics (Hecht, Laser Focus World, Apr 2011). Foundational reference for WPE improvement trajectory. [58]
2016	Measured, Laser Only	51.2%	IPG Photonics Yb:fibre laser at 10 kW class, laboratory demonstration. Primary anchor for Sub-model A baseline. V. Gapontsev et al [41]
2017	Measured, Laser Only	>43%	Lockheed Martin spectral-beam-combined fibre laser at 60 kW class, delivered to US Army. Confirms WPE improvement holds at higher power. Programme-reported, not a controlled laboratory measurement.
2019	Measured, Installed	~33%	Shipboard HEL system implied value: 150 kW output / 450 kW electrical draw (USNI News). Derived from reported figures, not a direct field measurement.
2021–2024	Measured, Installed	~35%	Military ground HEL systems, field operating conditions. Modelled engineering estimate; no published direct field measurement found in open sources. Corroborated by Karkadakattil [1], who reports system-level WPE of 20–35% for mobile military platforms. The lower bound of that range reflects less mature systems; the 33–35% figure adopted here aligns with the [44] shipboard measurement. Derived from laboratory WPE minus penalties for power conditioning, thermal derating, and ancillary loads. [1]
2024	Measured, Laser Only	~52%	Witte et al., near-laboratory conditions, 10–30 kW [43] Current state-of-art upper range for Yb:fibre under near-military conditions.
2025	Measured, Installed	~35%	JS Asuka (JMSDF) shipboard laser, ~100 kW, secondary source (LiveScience, Dec 2025). Range only, no direct measurement cited. Confirms military systems remain well below laboratory peak WPE.

Appendix Table A3: Component power budget model for vehicle-mounted HEL systems. All values are for the vehicle DC bus in a hybrid electric architecture. The laser-only WPE of 50% is measured at the laser head terminals; the chiller and all other loads draw separately from the same bus.

Component	Active during	Dependence on laser power	Notes
DE Source (laser chain)	Firing only	Linear with laser power	The laser chain is the dominant consumer. Wall-plug efficiency (WPE) is 50% at the laser head boundary, per Gapontsev et al. [41]. This figure excludes the chiller. Input power = laser output / WPE.
Vapour-compression chiller (optics cooling)	Firing and recovery	Linear with waste heat; waste heat is linear with laser power	The chiller must remove waste heat generated by the laser. Waste heat = laser electrical input minus laser output. Chiller electrical demand = waste heat / COP. The chiller runs continuously, including during non-firing phases, to drain the PCM thermal store.
Coolant pumps	Firing and recovery	Linear (3% of chiller load)	Centrifugal pumps circulating coolant through the laser head and chiller. Engineering estimate; no published figure for military systems. Insensitive parameter.
Beam director drive (tracking mode)	Firing; 0.5 kW idle during non-firing	Sub-linear with laser power	Power to drive the beam director gimbal in closed-loop tracking. Scales sub-linearly because larger apertures require heavier gimbals but tracking rate requirements do not increase proportionally. Scaling exponent is an engineering estimate; the contribution is small at all classes.
ATP sensors, fire control, communications	Firing and recovery	Constant (class-independent)	Electro-optical/infrared acquisition and tracking sensors (~2.0 kW); fire control computer (~1.0 kW); communications and C2 interface (~0.5 kW). These fixed loads are significant at Class A but negligible relative to laser and chiller at Class C and above.

Appendix Table A4: HEL Specific Mass: Plotted Data Points

Year	Value (kg/kW)	Description
~2013	~5.0	Excalibur coherent beam-combined fibre array (DARPA), demonstrated on MQ-9 Reaper. Laser subsystem only; ram-air cooled, no PTMS.
~2015	≤5.0	HELLADS programme target, DARPA / General Atomics, 150 kW aircraft integration. Laser subsystem only; no PTMS. Together with Excalibur, anchors the ~5 kg/kW aircraft benchmark.
2019	≤68.0	HELWS (Raytheon) on Polaris MRZR-D4 ultralight tactical vehicle, 10 kW output. First fully fielded ground system. Upper bound from vehicle payload limit (680 kg).
2022	≤55.1	DE M-SHORAD (Raytheon / US Army) on Stryker ICV (Infantry Carrier Vehicle) 8×8 wheeled APC (Armoured Personnel Carrier), 50 kW output. Upper bound from payload; note payload verification caveat in dataset.
2022	≤45.4	HEL-TVD (US Army High Energy Laser Tactical Vehicle Demonstrator) on FMTV M1083 6×6 5-ton cargo truck, 100 kW output. Clean payload envelope.

Aircraft points exclude PTMS and ruggedisation; they are not directly comparable to vehicle-mounted figures. Vehicle-mounted values are upper bounds from host-vehicle payload limits; true system mass lies at or below each value.

Appendix Table A5: HEL Engagement Feasibility Thresholds

Combines model-derived (Section A) and programme-confirmed (Section B) evidence. Row shading: yellow = model-derived (M); blue = programme-confirmed (P); green = consistent model prediction and programme evidence (M+P). Where model and programme evidence coincide at the same power level, they are merged into a single M+P row. DragonFire (FT-P9) is placed at estimated power class.

ID	Source / System	Output Power (kW)	Dwell Time (s)	Engage-ment Range (km)	Target Threats Neutralised	Ref
FT-T1	Fluence model — optical sensor / seeker defeat	5	0.5	3.0	Optical sensors, IR seekers, EO/IR camera arrays, radar radomes. Photonic overload of detector array. Required fluence ≤ 10 J/cm².	[40]
FT-P1	Rafael Lite Beam / JLTV (IDF (Israel Defense Forces), 2025)	10	N/C	N/C	Group 1 UAS; RPG (Rocket-Propelled Grenade). IDF operational service confirmed May 2025.	[61]
FT-P2	Raytheon HELWS / Wolfhound 6×6 (British Army, Porton Down, Jul 2024)	15	N/C	N/C	Group 1–2 UAS; drone targets. First live HEL firing from a UK military vehicle.	[6], [7]
FT-P3	Raytheon HELWS / JLTV (USAF (United States Air Force)/AFSOC (Air Force Special Operations Command), 2019 onwards)	15	N/C	N/C	Group 1–2 UAS. Operational USAF/AFSOC deployment; drone defeats confirmed.	[6][7]
FT-T2	Fluence model — drone avionics defeat	20	3	1.0	Drone avionics and flight-control electronics via composite airframe charring. Required fluence 50–200 J/cm².	[40]
FT-T3 / FT-P4	Fluence model + DE M-SHORAD / Stryker ICV (US Army, 2022–2023)	50	5 (model) N/C (prog.)	1.0 (model) N/C (prog.)	Group 1–3 UAS; FPV drones; loitering munitions; mortar rounds (RAM). Model: fluence 200–700 J/cm² for airframe structural defeat. Programme: mortar round defeat at operational engagement rates confirmed in DOT&E (Director, Operational Test and Evaluation) FY2024.	[40], [33], [59]
FT-P5	Lockheed Martin HELIOS Mk 5 / USS Preble (USN, Feb 2026)	60	N/C	N/C	Small UAS drone swarm: four drones defeated in a single engagement. Confirms 60 kW-class maturity for anti-UAS.	[35]
FT-T4	Fluence model — fuel system ignition	100	6	2.0	Fuel tank ignition (aluminium or composite tank). Required fluence 300–700 J/cm². Applicable to UAVs, rockets, and light vehicles with exposed fuel systems.	[40]
FT-P6	THEL / Nautilus chemical DF laser (US Army–Israel MoD, White Sands, 1996–2004)	100 (chemical)	~4 (est.)	~5.0 (est.)	Katyusha 122 mm rockets; 81 mm and 120 mm mortar rounds; artillery shells. Over 150 successful intercepts. DF chemical laser at 3.8 µm — not directly comparable to modern Yb:fibre systems. Historical existence proof.	[60]
FT-P7	Rafael Iron Beam 450 / Tatra T815-7 8×8 (Israel, AUSA 2024)	~100	N/C	N/C	Rockets; mortars; ATGMs (Anti-Tank Guided Missiles); small UAS. IDF operational service confirmed May 2025.	[61]
FT-T4b / FT-P8	Fluence model + DARPA HELLADS (aircraft, ~2015–2017)	150	6 (model) N/C (prog.)	2.0 (model) N/C (prog.)	Rocket/mortar body defeat (model). Ground tests at White Sands against rocket targets confirmed (programme). Aircraft laser subsystem: < 5 kg/kW demonstrated.	[40, 36]

ID	Source / System	Output Power (kW)	Dwell Time (s)	Engage-ment Range (km)	Target Threats Neutralised	Ref
FT-T5 / FT-T6	Fluence model — rocket/mortar defeat and missile guidance defeat	200	3–5	2.0–3.0	Thin-steel rocket/mortar body (fluence 500–2,000 J/cm²) and missile guidance head defeat (fluence 700–2,000 J/cm²). At 200 kW the same system is capable of addressing both target categories depending on dwell.	[40]
FT-P9	MBDA DragonFire (Royal Navy/UK MoD, trials Oct–Nov 2025)	~30–50 (est.)	"seconds" (N/C)	N/C	Fast-moving drone targets including 650 km/h class. Multiple confirmed kills. Production contract £316 million. Cost per engagement ~£10. Output power not released in open sources.	[7]
FT-T7	Fluence model — cruise missile airframe defeat	500	10	3.0	Cruise missile and large UAV airframe structural defeat. Required fluence 2,000–5,000 J/cm². Military cruise missiles may carry ablative coatings to resist burn-down.	[40]
FT-T8	Fluence model — manned aircraft / rotary-wing kill	500	20	5.0	Manned fixed-wing aircraft and supersonic cruise missiles with ablative coatings at operationally relevant ranges; requires extended dwell of 20–30 s. Ballistic missile boost-phase intercept is excluded from ground vehicle analysis as it requires an airborne or space-based platform at 300–500 km standoff.	[40]

Notes: M = model-derived (Zohuri [40] fluence model + Note 3 aperture/atmospheric model). P = programme-confirmed in open-source literature. M+P = consistent model prediction and programme evidence. N/C = not confirmed in open-source literature. Power values for M rows are minimum thresholds at stated dwell and range; actual deployed system power will exceed these values. THEL (FT-P6) uses DF chemical laser at 3.8 μm — not directly comparable to 1.07 μm Yb:fibre systems. "~" = estimate from programme context.

Appendix Table A6: HEL Fluence Physics: Basis for Class A–E Boundaries.

This table provides the physics derivation underpinning the Class A–E power boundaries defined in Section 3.4 and Table 3. Power, dwell time, and engagement range derived from this fluence basis are tabulated in Table A (threshold register). The fluence and energy loss values are sourced from Zohuri [40]; engagement range estimates use the aperture/atmospheric model of Note 3.

Class (kW)	Target Category	Required Fluence at Target (J/cm²)	Primary Defeat Mechanism	Combined Energy Loss[1] Initial → Sustained	Notes
A 20 kW	Optical sensors, IR seekers, EO/IR camera arrays, radar radomes (seeker dazzle / photonic kill); Group 1–2 UAS composite airframe (avionics defeat)	≤ 10 (seeker dazzle) 50–200 (avionics / airframe)	Photonic overload of detector array — no surface ablation required (seeker). Composite avionics / airframe charring; absorptance rises from ~25% to ~70% as CFRP (Carbon Fibre Reinforced Polymer) chars within 1–2 s of dwell (UAS).	60–75% throughout (seeker — glass/plastic dome does not char). 65–80% initial → 40–60% sustained (UAS airframe).	Seeker defeat does not require dwell; UAS airframe defeat does. Class A is the only class with two physically distinct mechanisms at the same power level. Demonstrations: HELWS 15 kW on Wolfhound / JLTV [6],[7]; Rafael Lite Beam 10 kW on JLTV [61]; Rheinmetall Skyranger 30 HEL 20 kW on Boxer (Bundeswehr) [26]
B 60 kW	Group 3 UAS and one-way attack drones (Shahed-136 class); mortar rounds (81–120 mm) in flight	200–700 (large UAS airframe) 500–2,000 (thin steel mortar body)	Composite structural failure by delamination or burn-through (UAS). Steel body heating and propellant / explosive ignition (mortar); mill-scale and paint burn off rapidly, raising steel absorptance sharply.	65–75% initial → 30–50% sustained (CFRP carbonises; surface becomes near-black). 65–75% initial → 35–55% sustained (steel; absorptance rises with surface temperature).	Upper end of fluence range (700 J/cm² UAS; 2,000 J/cm² mortar) requires higher dwell or closer range; Class B power at 50 kW accommodates both at operationally relevant ranges. Demonstrations: DE M-SHORAD 50 kW on Stryker — DOT&E vs. Group 3 UAS and mortars [33],[59]; HELIOS Mk 5 Mod 0, 60 kW, USS Preble — vs. UAS swarm, Feb 2026 [35]
C 150 kW	122 mm rockets in flight; unprotected cruise missiles (non-ablative airframes); fuel system ignition (aluminium or composite tanks)	300–700 (fuel ignition) 500–2,000 (rocket body) 2,000–5,000 (cruise missile airframe)	Fuel tank ignition — paint burns off in ~1 s exposing bare metal or composite; aluminium remains more reflective than composites throughout. Steel rocket body structural defeat	70–85% initial → 45–65% sustained (aluminium fuel tank; retains reflectance). 65–75% initial → 35–55% sustained (steel rocket body). 65–75% initial → 35–55% sustained (cruise missile;	Ablative missile coatings (deliberate engineering countermeasure) can maintain high reflectance throughout engagement,

Class (kW)	Target Category	Required Fluence at Target (J/cm²)	Primary Defeat Mechanism	Combined Energy Loss[1] Initial → Sustained	Notes
			(same mechanism as Class B but higher fluence required for thicker bodies). Cruise missile airframe structural defeat — mixed metal/composite construction.	ablative coatings if present resist burn-down by design).	preventing the burn-down effect. Class C is defined to defeat non-ablative cruise missiles; hardened ablative threats fall to Class D. Demonstrations: DARPA HELLADS 150 kW (aircraft) [37]; Rafael Iron Beam ~100 kW on Tatra [61]
D 300 kW	Cruise missiles with ablative coatings (engineered countermeasure); rotary-wing aircraft (helicopter structural kill); hardened RAM (thick-wall steel rockets)	2,000–5,000 (ablative cruise missile) 5,000–10,000 (rotary-wing structure)	Sustained ablation through surface countermeasure — laser must continuously ablate the protective coating faster than it regenerates. Rotary-wing structural kill via rotor head and fuel system aimpoints; long dwell required.	20–50% throughout (ablative coating sheds material continuously; fresh high-reflectance surface presented to beam). 65–80% initial → 35–55% sustained (rotary-wing aluminium/composite structure).	Ablative coating defeat requires maintaining irradiance above the ablation threshold continuously; any break in lock allows coating to regenerate. Target may also manoeuvre to break laser lock during long dwell. Demonstrations: IFPC-HEL / Valkyrie programme specification >250 kW
E 50 0 kW	Manned fixed-wing aircraft (structural kill); supersonic cruise missiles with heavy ablative coatings	5,000–10,000 (fixed-wing structure) ≥ 5,000 (ballistic missile, ablative)	Deep structural kill — sustained ablation through thick aluminium or composite skin; preferred aimpoints are fuel system and control surfaces. Ballistic missile boost-phase intercept — thin atmosphere (airborne platform) reduces propagation loss but ablative nose cone presents continuously fresh surface.	65–80% initial → 35–55% sustained (fixed-wing structure; full surface modification with sustained dwell). 20–40% throughout at altitude (thin atmosphere reduces propagation loss; ablative coating maintains high reflectance by design).	Fixed-wing target may manoeuvre and break laser lock during the long dwell required. Rotor head and fuel system are preferred aimpoints for rotary-wing (Class D) and fuel system / control surfaces for fixed-wing (Class E). Ballistic missile boost phase requires an airborne or space-based platform at standoff range of 300–500 km. Fluence model FT-T8 [40]. Demonstrations: YAL-1 Airborne Laser programme (~1 MW)

Notes

1. Fluence (J/cm²) is energy absorbed per unit area at the aimpoint. For irradiance I (W/cm²) and dwell time t (s): F = A × I × t, where A is the surface absorptance fraction (typically 0.20–0.60 at initial contact, rising to 0.70–0.90 as surface chars or oxidises). Fluence values are thresholds for functional kill of a representative target in each class; actual values vary with target construction, orientation, and atmospheric path.
2. Combined energy loss = 1 − (energy performing useful thermal work on target) / (laser emitted power). Typical breakdown: atmospheric transmission 30–50%; beam quality and pointing 10–20%; surface reflectance 20–80% depending on material and dwell phase. "Initial" applies at beam-on; "sustained" applies after surface modification (charring, oxidation, or ablation) has occurred. The burn-down effect — rising absorptance with dwell — is beneficial for uncoated targets; ablative coatings are engineered to prevent it.
3. Engagement range estimates (in Table A) assume: aperture 30 cm; wavelength 1.07 μm (ytterbium fibre laser); $M^2 \leq 1.3$; atmospheric transmission 70% at sea level under moderate conditions. CO_2 (10.6 μm) systems such as THEL require approximately 10× greater aperture area or output power to achieve equivalent irradiance at the same range, due to stronger atmospheric absorption at 10.6 μm. All range values in Table A are derived quantities from this model; they are not citable data from field trials.
4. The burn-down effect means total energy-to-kill is lower than a fixed-reflectance calculation implies, because rising absorptance delivers more useful thermal power per unit of laser output as dwell continues. Ablative missile coatings (Classes C–E) are specifically engineered to prevent this effect by shedding the charred surface layer continuously, maintaining high reflectance throughout the engagement. This is the principal physical reason that Classes D and E require substantially higher power than the fluence values alone would suggest.
5. Source: Zohuri [40]

Appendix Table A7: Step-by-step derivation of the adopted chiller COP.

Parameter	Value	Derivation and basis
Laser coolant return temperature (heat source, T_cold)	**20°C**	Representative inlet temperature for a fibre laser diode coolant loop. Diode arrays require coolant well below 30°C to prevent thermal derating. Using 20°C is a mid-range engineering estimate; a higher value would increase COP (less work required), so this choice is slightly conservative.
Heat rejection temperature (T_hot)	**60°C**	MIL-STD-810G, Method 501.7, [50] Hot-Dry cycle specifies a maximum 24-hour average air temperature of 49 degrees C for equipment qualification in arid/hot environments [48]. The condenser must reject heat to this ambient air; it does so through a heat exchanger that requires a temperature difference between the refrigerant and the air to drive the heat transfer. An approach temperature of 10 to 15 K is standard in industrial chiller design practice, representing the minimum driving difference achievable with a compact condenser coil of practicable size. Using 11 K gives T_hot = 49 + 11 = 60 degrees C. This is a conservative (slightly high) estimate; a larger condenser would reduce the approach temperature and improve COP, so the adopted value errs toward lower efficiency.
Theoretical maximum COP (Carnot COP)	**7.33**	The Carnot COP is the upper bound for any refrigeration cycle operating between T_cold and T_hot. It equals T_cold (in Kelvin) divided by the temperature lift (T_hot minus T_cold in Kelvin): 293 K / (333 K minus 293 K) = 293 / 40 = 7.33. See, for example, Cengel and Boles, Thermodynamics: An Engineering Approach, McGraw-Hill, current edition, Section 6-5. No real chiller achieves the Carnot limit.
Practical efficiency fraction (real / Carnot)	**51%**	Military and industrial vapour-compression chillers operating at moderate temperature lifts (25–35 K) typically achieve 45–55% of the Carnot COP, depending on compressor type and refrigerant. The 51% figure is consistent with published data for scroll and reciprocating compressor systems in this operating regime.
Adopted COP	**3.7**	COP = 51% of Carnot COP = 0.51 × 7.33 = 3.74, rounded to 3.7.

T_cold = 20 degrees C is the laser coolant return temperature; T_hot = 60 degrees C is the condenser temperature, equal to the MIL-STD-810G worst-case ambient plus an 11 K approach temperature. The Carnot COP is the thermodynamic upper bound; real vapour-compression chillers typically achieve 45 to 55 per cent of this limit (51 per cent adopted as an engineering estimate).

Appendix Table A8: HEL Dwell Time (t_dwell) by Class — Derivation from Fluence Threshold Register

Class	P_laser (kW)	t_dwell central (s)	Sensitivity range (s)	E_shot (kJ)	Source row
A	20	3	1–5	60	FT-T2 (Zohuri fluence model)
B	60	5	3–8	300	FT-T3 scaled (model + DE M-SHORAD programme)
C	150	6	4–10	900	FT-T4b (model + HELLADS programme)
D	300	17	10–30	5,100	FT-T7 scaled (model only; no programme confirmation)
E	500	30	20-40	15,000	FT-T8

Notes:

E_shot = P_laser × t_dwell (kill energy per shot at the primary target type for each class).

t_dwell values are derived from Table A5 fluence threshold register (Zohuri [40]).

Confidence ratings reflect data source quality: MED-HIGH = model-derived with independent programme corroboration at the same power class; MEDIUM = model row with partial programme support or power scaling applied; LOW = model only, no open-source programme confirmation.

Appendix Table A9: DEW subsystem specific mass at 100 kW output. EPS is reduced relative to a standalone system because the hybrid DC bus provides battery storage and stabilised supply voltage.

Subsystem	kg/kW (low)	kg/kW (high)	Basis / Source
DE Source (laser, pump diodes, SBC combiner, output optics to BD aperture)	4.4	5.0	RELI/LM 2017 (~5 kg/kW at 60 kW) and HELLADS LWM (~4.0 kg/kW at 150 kW) data points scaled to 100 kW.
Thermal Management / PTMS (liquid loop, pump, HX, PCM store, vehicle-side HX)	2.0	2.8	Sharar, Jankowski & Morgan, ARL DTIC ADA529968 (2010) [62]
Beam Director (steerable telescope, gimbal, ruggedised MIL-STD-810)	2.0	4.0	200–400 kg estimated for 30–50 cm aperture stabilised telescope, consistent with the HEL TVD minimum aperture specification (SMDC). Comparable to vehicle-mounted EO/IR turrets of similar aperture.
ATP Sensors (EO/IR tracker, radar cue receiver, processor)	0.5	1.5	50–150 kg for EO/IR tracking sensor plus radar cue receiver. Fixed overhead, power-class independent.
Platform Integration (mounts, EMI shielding, harness, connectors, armoured housing)	0.5	1.5	50–150 kg fixed overhead; power-class independent. Allowance for MIL-STD-810 mechanical integration, MIL-STD-461 EMI shielding, cable harness and connectors, and armoured housing panels.
EPS / Power Conditioning (DC-DC converter, EMI filter, isolation transformer)	0.5	1.0	100–200 kg for military-ruggedised DC-DC conversion at 100 kW, halved relative to a standalone system because the hybrid powertrain DC bus already provides battery energy storage and a stabilised supply voltage, eliminating the AC front-end.
Fire Control and Track Manager (ruggedised processor and I/O)	0.2	0.5	20–50 kg. Power-class independent. Treated as mass-negligible in the platform feasibility analysis.
Beam Transport (internal fibre, DE Source to BD aperture)	0.1	0.2	~10–20 kg short internal fibre run. Negligible.
TOTAL	**10.2**	**16.5**	**Sum of subsystem low and high estimates.**

8. REFERENCES

[1] Karkadakattil, A., "Laser-Based Directed Energy Weapons: Technological Capabilities, Material Interaction, and Strategic Deployment Pathways," *Defence Science Review*, No. 21, 2025 (received Dec. 2025; accepted Jan. 2026). DOI: https://doi.org/10.37055/pno/216776 (accessed on March 9, 2026).

[2] UK Ministry of Defence, "DragonFire directed energy weapon: £10 per shot laser capability", MoD press release, November 2025. Available at: https://www.gov.uk

[3] UK Ministry of Defence, "British Army successfully tests new drone-destroying laser", MoD press release, December 2024. Available at: https://www.gov.uk/government/news/british-army-successfully-tests-new-drone-destroying-laser

[4] UK Strategic Defence Review, March 2025, HM Government, London. (Report: SDR directed energy investment, ~£1 billion commitment)

[5] A. White, "RTX's HELWS anti-drone laser weapon looking for new use cases," *Breaking Defense*, Jul. 21, 2025. Available: https://breakingdefense.com/2025/07/rtxs-helws-anti-drone-laser-weapon-looking-for-new-use-cases/ (accessed Mar. 11, 2026).

[6] Defence Equipment and Support / Raytheon UK, "Raytheon HELWS completes live-firing with British Army", December 2024. Reported in: European Security & Defence, Vol. 23, December 2024.

[7] Navy Lookout, "DragonFire – pathway to a Laser Directed Energy Weapon for the Royal Navy?" March 2024. URL: https://www.navylookout.com/dragonfire-pathway-to-a-laser-directed-energy-weapon-for-royal-navy/ (accessed March 2026).

[8] UK Defence Equipment and Support (DE&S), "Preliminary Market Engagement Notice: Land Laser Directed Energy Weapon (LDEW)", FMC-StratProgs-CWDEW-Group@mod.gov.uk, 13 June 2025.

[9] Office of Naval Research, "Directed Energy Weapons: High Power Microwaves," ONR Division 353, 2022. URL: https://www.onr.navy.mil/organization/departments/code-35/division-353/directed-energy-weapons-high-power-microwaves (accessed March 3, 2026).

[10] Headquarters, Department of the Army, *Field Artillery Manual Cannon Gunnery*, Training Circular TC 3-09.81, Washington, DC: US Government Publishing Office, April 2016. Available: https://armypubs.army.mil/epubs/DR_pubs/DR_a/pdf/web/tc3_09x81.pdf (accessed March 17, 2026).

[11] Congressional Research Service, "Department of Defense Directed Energy Weapons: Background and Issues for Congress," CRS Report R46925, updated 2024. Available: https://www.congress.gov/crs-product/R46925

[12] Silvas, E.; Hofman, T.; Murgovski, N.; Etman, L.F.P.; Steinbuch, M. Review of Optimization Strategies for System-Level Design in Hybrid Electric Vehicles. *IEEE Transactions on Vehicular Technology*, 2017, 66(1), 57–70. DOI: 10.1109/TVT.2016.2547897 (accessed March 18, 2026).

[13] Zaki, M.I. et al. "Development of vehicle powertrain simulation module by interfacing Matlab-ADVISOR to LabVIEW." *ResearchGate*, 2017. (accessed March 18, 2026).

[14] R. Tull de Salis, "Rapid Evaluation of Off-Highway Powertrain Architectures," *World Electr. Veh. J.*, vol. 16, no. 12, p. 671, Dec. 2025, doi: 10.3390/wevj16120671.

[15] S. Zulkifli and M. A. Mohd. Dali, "Development of vehicle powertrain simulation module by interfacing Matlab-ADVISOR to LabVIEW," in *Proc. 2017 IEEE Conference on Systems, Process and Control (ICSPC)*, Melaka, Malaysia, Dec. 2017, doi: 10.1109/SPC.2017.8313034.

[16] Kramer, D.M.; Parker, G.G. Current State of Military Hybrid Vehicle Development. Int. J. Electric Hybrid Veh. 2011, 3, 369–387. https://doi.org/10.1504/IJEHV.2011.044373.

[17] Wikipedia contributors, "Ocelot (vehicle)," *Wikipedia*, last modified November 2025. Available: https://en.wikipedia.org/wiki/Ocelot_(vehicle) (accessed 12 March 2026).
[18] GlobalData / Army Technology, "Foxhound Light Protected Patrol Vehicle (LPPV), UK," *Army Technology*, updated January 2026. Available: https://www.army-technology.com/projects/ocelot-lppv/ (accessed Mar. 11, 2026).
[19] Morrison, B., "Armour Focus: Foxhound LPPV Pt 3," *Joint Forces News*, Dec. 2022. Available: https://www.joint-forces.com/features/18750-armour-focus-foxhound-lppv-pt-3 (accessed Mar. 11, 2026).
[20] Army Recognition, "Analysis: Discover Wolfhound MRAP vehicle donated by UK to Ukraine," Army Recognition, May 2022. Available: https://www.armyrecognition.com/focus-analysis-conflicts/army/conflicts-in-the-world/russia-ukraine-war-2022/analysis-discover-wolfhound-mrap-vehicle-donated-by-uk-to-ukraine (accessed Mar. 13, 2026).
[21] Army Technology, "Mastiff 2 Protected Patrol Vehicle," army-technology.com/projects/mastiff-2/ (accessed Mar. 13, 2026).
[22] Rheinmetall BAE Systems Land (RBSL), "UK Boxer MIV programme update", Telford, January 2024. Available at: https://www.rheinmetall.com/en/media/news-watch/news/2024/01/2024-01-23-rheinmetall-boxer-miv-update
[23] European Security & Defence, "UK Boxer Programme Moves Ahead", Vol. 21, September 2022.
[24] RBSL / Rolls Royce, "MTU 8V 199 TS21 engine selected for UK Boxer MIV", RBSL press release, 3 August 2022. (600 kW rating)
[25] US Army / GDLS, "Stryker A1 ICT vehicle: Caterpillar C9 engine, 450 hp (335 kW)", US Army Factsheet, undated. Available at: www.army.mil
[26] Rheinmetall AG, "The Skyranger 30 HEL — Rheinmetall's hybrid solution for threat-commensurate, modern mobile air defence," press release, 4 February 2022. Available: https://www.rheinmetall.com/en/media/news-watch/news/2022/2022-02-04_the-skyranger-30-hel (accessed 12 March 2026).
[27] T. Podlesak, "Radio Frequency Directed Energy Weapon Design Tool," DSIAC Journal, 2022. URL: https://dsiac.dtic.mil/articles/radio-frequency-directed-energy-weapon-design-tool/(accessed March 3, 2026).
[28] N. Sherwood, "Radio Frequency Directed Energy Weapon with Potential Naval Applications Successfully Demonstrated in the UK," Navy Lookout, Feb. 2025. Available: https://www.navylookout.com/radio-frequency-directed-energy-weapon-with-potential-naval-applications-successfully-demonstrated-in-the-uk/ (accessed Mar. 3, 2026).
[29] P. Dussinger, "Thermal Management for Directed Energy Weapons," *Mobility Engineering Technology* (SAE Media Group), September 2020. Available: https://www.mobilityengineeringtech.com/component/content/article/37608-thermal-management-for-directed-energy-weapons (accessed 12 March 2026).
[30] P. Ritt, D. Pellicone, and H. Pearlman (Advanced Cooling Technologies, Inc.), "Compact Thermal Management Solutions for Mobile Laser Weapon Systems," *Mobility Engineering Technology* (SAE Media Group), 2015. Available: https://www.mobilityengineeringtech.com/component/content/article/23128-compact-thermal-management-solutions-for-mobile-laser-weapon-systems (accessed 12 March 2026).
[31] AeroVironment, Inc., "AV Delivers JLTV-Mounted LOCUST Laser Weapon Systems to U.S. Army," press release, Arlington, VA, Dec. 18, 2025 Available: https://investor.avinc.com/news-releases/ news-release-details/av-delivers-jltv-mounted-locust-laser-weapon- systems-us-army (accessed Mar. 2026).
[32] Lockheed Martin Corporation, "Turning Up the Heat: Latest Evolution of Lockheed Martin Laser Weapon System Stops Truck in Field Test," press release, 3 March 2015. Available:

https://news.lockheedmartin.com/2015-03-03-Turning-Up-the-Heat-Latest-Evolution-of-Lockheed-Martin-Laser-Weapon-System-Stops-Truck-in-Field-Test (accessed on March 13, 2026).

[33] US Army / Congressional Research Service, "U.S. Army Maneuver Short-Range Air Defense (M-SHORAD) System," CRS In Focus IF12397, updated 2025. Available: https://www.congress.gov/crs-product/IF12397

[34] Lockheed Martin Corporation, "Lockheed Martin Delivers Integrated Multi-Mission Laser Weapon System to the Navy," press release, 18 Aug. 2022. Available: https://news.lockheedmartin.com/2022-08-18-Lockheed-Martin-Delivers-Integrated-Multi-Mission-Laser-Weapon-System-to-the-Navy (accessed Mar. 17, 2026).

[35] Trevithick, J. (2026, Feb. 3). "USS Preble Used HELIOS Laser To Zap Four Drones In Expanding Testing." The War Zone. twz.com/sea/uss-preble-used-helios-laser-to-zap-four-drones-in-expanding-testing (Accessed Mar. 2026).

[36] DARPA. (2015). "HELLADS: High Energy Liquid Laser Area Defense System." Programme overview. darpa.mil (Accessed Mar. 2026).

[37] General Atomics Aeronautical Systems, Inc. (2015, May 21). "HELLADS Laser Completes Development." Press release. Available: https://www.ga.com/hellads-laser-completes-development (accessed Mar. 11, 2026).

[38] W. Roscello et al. (The MITRE Corporation / OUSD(R&E)), "An Overview of the Directed Energy Weapon Systems Modular Open Systems Approach Reference Architecture (DEWS MOSA RA)," NDIA Ground Vehicle Systems Engineering and Technology Symposium (GVSETS) 2022, Distribution A: Approved for Public Release. Available: https://ndia.dtic.mil/wp-content/uploads/2022/systems/Wed_24609_Roscelloe.pdf

[39] J. Vetrovec and R. Rice, "Thermal Management System for Solid-State High-Energy Laser," in *Proc. 15th Annual Solid-State and Diode Laser Technology Review*, Directed Energy Professional Society, 2002. https://www.researchgate.net/publication/244987464 (accessed 12 March 2026)

[40] Zohuri, B. (2016). Directed Energy Weapons: Physics of High Energy Lasers (HEL). Springer International Publishing, Cham. ISBN 978-3-319-31289-7. (Fluence-to-kill thresholds, Sections A and C of tables.)

[41] Gapontsev, V., Shcherbakov, E., Fomin, V., Abramov, A., Abramov, M., Ferin, A., Mironov, V., and Doronkin, A. (IPG Photonics), "Multi-Kilowatt CW Fiber Laser Systems with Record Wall-Plug Efficiency Exceeding 50%," in *Proc. 2016 International Conference Laser Optics (LO 2016) / 8th International Symposium on High-Power Fiber Lasers and Their Applications*, St. Petersburg, Russia, 27 Jun.–1 Jul. 2016. Available: https://www.researchgate.net/publication/305209000 (accessed on March 9, 2026).

[42] Lockheed Martin Corporation, "Lockheed Martin to Deliver World Record Setting 60kW Laser to U.S. Army," press release, 16 Mar. 2017. Available: https://news.lockheedmartin.com/2017-03-16-Lockheed-Martin-to-Deliver-World-Record-Setting-60kW-Laser-to-U-S-Army (accessed on March 9, 2026).

[43] Witte, U. et al. (Laserline GmbH), "Multi-10kW diode laser systems with wall-plug efficiency greater than 50%," *Proc. SPIE 13345, High-Power Diode Laser Technology XXIII*, 133450H, 21 Mar. 2025. DOI: https://doi.org/10.1117/12.3048960 (accessed on March 9, 2026).

[44] LaGrone, S., "Navy to Field High Energy Laser Weapon, Laser Dazzler on Ships This Year," *USNI News*, 30 May 2019. Available: https://news.usni.org/2019/05/30/navy-to-field-high-energy-laser-weapon-laser-dazzler-on-ships-this-year (accessed on March 9, 2026).

[45] National Research Council, *Selected Directed Energy Research and Development for U.S. Air Force Aircraft Applications: A Workshop Summary*. Washington, DC: The National Academies Press, 2013. DOI:

https://doi.org/10.17226/18497. Available: https://nap.nationalacademies.org/catalog/18497 (accessed Mar. 11, 2026).

[46] Defense Advanced Research Projects Agency (DARPA), "High Energy Liquid Laser Area Defense System (HELLADS)," in *Department of Defense Fiscal Year 2013 President's Budget: Research, Development, Test and Evaluation, Defense-Wide*, Program Element 0602702E, Office of the Under Secretary of Defense (Comptroller), Feb. 2012. Available: https://comptroller.war.gov/Portals/45/documents/defbudget/fy2013/budget_justification/pdfs/03_RDT_and_E/Defense_Advanced_Research_Projects_Agency_PB_2013_1%20Final.pdf (accessed Mar. 11, 2026).

[47] Skeleton Technologies GmbH, "SkelMod 162V62F Ultracapacitor Module," Product Datasheet, Doc. No. 01-DS-240124-SKELMOD-162V62F-1D, January 2024. Available: https://www.skeletontech.com/hubfs/Data_sheets/Modules/DS-SKELMOD-162V62F-240124.pdf (accessed March 17, 2026).

[48]: PMC7516462 — R-134a automotive AC experimental COP data (pmc.ncbi.nlm.nih.gov/articles/PMC7516462/)

[49]: Brown et al. — NIST publication 860836, R-134a benchmark COP at 32°C ambient (tsapps.nist.gov/publication/get_pdf.cfm?pub_id=860836)\

[50] (MIL-STD-810G) Department of Defense, *MIL-STD-810G: Environmental Engineering Considerations and Laboratory Tests*, Department of Defense, Washington, DC, USA, 31 Oct. 2008.

[51]: Yang et al., MDPI Aerospace 2025, 12(8) 681, DOI 10.3390/aerospace12080681 — Boeing 787 galley CRU 83 kg / 15 kW(thermal)

[52]: Sanden SD7H15 Service Guide Rev 2 (sanden.com) — compressor 8.0 kg, capacity ~7.6 kW(thermal)

[53]: Classic Retrofit Electrocooler product data (classicretrofit.com) — complete circuit under 15 kg

[54]: Thermo King Athenia AM II 1000 datasheet — 213 kg, 26–31 kW(thermal)

[55]: Mobile Climate Control Reference Manual 2014 (bcc-hvac.com) — evaporator units 27 kg/8 kW and 43 kg/14 kW (ARI conditions)

[56] Tull de Salis, R., "A Standardised Mission Profile and Rapid Architecture Screening Methodology for Hybrid-Electric Tactical Wheeled Vehicles," in Proc. 2026 Ground Vehicle Systems Engineering and Technology Symposium (GVSETS), Novi, MI, Aug. 2026 (companion paper, submitted simultaneously).

[57] Khalil, G.; Danielson, E.; Barshaw, E.; Chait, M., "Weapon and Armor System Power in Future Combat Vehicles", SAE Technical Paper / Mobility Engineering Technology, US Army TARDEC, Warren, MI, 2017.

[58] Hecht, J., "Photonic Frontiers: High-Efficiency Optical Pumping," *Laser Focus World*, Apr. 2011. Available: https://www.laserfocusworld.com/lasers-sources/article/16547048 (accessed on March 9, 2026).

[59] Director of Operational Test and Evaluation (DOT&E). (2024). FY2024 Annual Report — DE M-SHORAD. Office of the Secretary of Defense, Washington DC. Available: dote.osd.mil/Portals/97/pub/reports/FY2024/army/2024de_m-shorad.pdf (Accessed Mar. 2026).

[60] Shwartz, J., Wilson, G.T., and Avidor, J.M. (2002). "Tactical high-energy laser." *Proc. SPIE 4632, Laser and Beam Control Technologies*, 4 June 2002. https://www.spiedigitallibrary.org/conference-proceedings-of-spie/4632/0000/Tactical-high-energy-laser/10.1117/12.469758.short (Accessed on March 11, 2026)

[61] GovConExec. (2025, Oct.). "Rafael Iron Beam Ready for Export, IDF Deployment in 2025." govconexec.com (Accessed Mar. 2026); Army Recognition. (2024, Oct.). "Rafael expands Iron Beam laser family with new mobile variant on Tatra chassis." AUSA Annual Meeting 2024. armyrecognition.com (Accessed Mar. 2026). Vehicle payload (Tatra T815-7 VT 8×8, 10,000 kg) from: Tatra Trucks a.s., T815-7 specification, tatra.cz (Accessed Mar. 2026).

[62] D. Sharar, N. R. Jankowski, and B. Morgan, "Review of Two-Phase Electronics Cooling for Army Vehicle Applications," U.S. Army Research Laboratory, Adelphi, MD, ARL Technical Report ARL-TR-5323, DTIC Accession No. ADA529968, Sep. 2010. https://apps.dtic.mil/sti/tr/pdf/ADA529968.pdf (accessed on March 19, 2026)

[63] D. Mehta, "Give 'Em E-HEL: Army Seeks Industry Ideas for Counter-Drone Laser Systems," *Breaking Defense*, 3 Nov. 2025. Available: https://breakingdefense.com/... (accessed Mar. 2026).

[64] DRDO / CHESS (Centre for High Energy Systems and Sciences), "India Demonstrates Laser Weapon Capability, Joins Elite Global Club," *News on Air* (All India Radio / Prasar Bharati), 13 Apr. 2025. Available: https://www.newsonair.gov.in/... (accessed March 2026).

9. CONTACT INFORMATION

Rupert Tull de Salis
ZeBeyond Ltd, Leamington Spa, UK
rdesalis@umich.edu

10. ACKNOWLEDGMENT

This work was funded by ZeBeyond Ltd.

11. ACRONYMS

ADS	Active Denial System
AESA	Active Electronically Scanned Array
AFSOC	Air Force Special Operations Command
APC	Armoured Personnel Carrier
ATGM	Anti-Tank Guided Missile
ATP	Acquisition, Tracking and Pointing
BEV	Battery Electric Vehicle
C-RAM	Counter-Rocket, Artillery and Mortar
C-UAS	Counter-Unmanned Aerial System
CEMP-H	Central European Mission Profile – Hybrid
CFRP	Carbon Fibre Reinforced Polymer
COP	Coefficient of Performance
CRS	Congressional Research Service
DC	Direct Current
DCDC	Direct Current to Direct Current (converter)
DE	Directed Energy
DEW	Directed Energy Weapon
DEWS	Directed Energy Weapon System
DOT&E	Director, Operational Test and Evaluation
EMI	Electromagnetic Interference
EO/IR	Electro-Optical/Infrared
EPS	Electrical Power System

FMTV	Family of Medium Tactical Vehicles
FPV	First-Person View
GVM	Gross Vehicle Mass
HEL	High Energy Laser
HELLADS	High Energy Liquid Laser Area Defense System
HELIOS	High Energy Laser with Integrated Optical-dazzler and Surveillance
HELWS	High Energy Laser Weapon System
HMI	Human Machine Interface
HPM	High-Power Microwave
HPPV	Heavy Protected Patrol Vehicle
ICE	Internal Combustion Engine
ICV	Infantry Carrier Vehicle
IDF	Israel Defense Forces
IFPC	Indirect Fire Protection Capability
JMSDF	Japan Maritime Self-Defense Force
JP-8	Jet Propellant 8
JLTV	Joint Light Tactical Vehicle
LPPV	Light Protected Patrol Vehicle
MGU	Motor Generator Unit
MIL-STD	Military Standard
MIV	Mechanised Infantry Vehicle
MMW	Millimetre Wave
MOSA	Modular Open Systems Approach
M-SHORAD	Maneuver Short-Range Air Defense
NATO	North Atlantic Treaty Organisation
OUSD(R&E)	Office of the Under Secretary of Defense for Research and Engineering
PCM	Phase Change Material
PTMS	Power and Thermal Management System
RAM	Rocket, Artillery and Mortar
RBSL	Rheinmetall BAE Systems Land
RELI	Robust Electric Laser Initiative
RFDEW	Radio Frequency Directed Energy Weapon
RPG	Rocket-Propelled Grenade
SBC	Spectral Beam Combining
SFF	Sustained Firing Fraction
SOC	State of Charge
TRL	Technology Readiness Level
UAS	Unmanned Aerial System
USAF	United States Air Force
VTOL	Vertical Take-Off and Landing
WPE	Wall Plug Efficiency